MICROCOPY RESOLUTION TEST CHART

NATIONAL BUREAU OF STANDARDS-1963-A

REPORT DOCUMENTATION PAGE		READ INSTRUCTIONS BEFORE COMPLETING FORM
1. REPORT NUMBER AFOSR-TR- 83-1336	**2. GOVT ACCESSION NO.** AD-A137029	**3. RECIPIENT'S CATALOG NUMBER**
4. TITLE (and Subtitle) A SYNTHESIZED MODEL OF THE NEAR-WALL BEHAVIOR IN TURBULENT BOUNDARY LAYERS		**5. TYPE OF REPORT & PERIOD COVERED** INTERIM
		6. PERFORMING ORG. REPORT NUMBER
7. AUTHOR(s) C R SMITH		**8. CONTRACT OR GRANT NUMBER(s)** F49620-78-C-0071
9. PERFORMING ORGANIZATION NAME AND ADDRESS LEHIGH UNIVERSITY DEPT OF MECHANICAL ENGINEERING & MECHANICS BETHLEHEM, PA 18015		**10. PROGRAM ELEMENT, PROJECT, TASK AREA & WORK UNIT NUMBERS** 61102F 2307/A2
11. CONTROLLING OFFICE NAME AND ADDRESS AIR FORCE OFFICE OF SCIENTIFIC RESEARCH/NA BOLLING AFB, DC 20332		**12. REPORT DATE** 1984
		13. NUMBER OF PAGES 27
14. MONITORING AGENCY NAME & ADDRESS(If different from Controlling Office)		**15. SECURITY CLASS. (of this report)** Unclassified
		15a. DECLASSIFICATION/DOWNGRADING SCHEDULE

16. DISTRIBUTION STATEMENT (of this Report)

Approved for Public Release; Distribution Unlimited.

17. DISTRIBUTION STATEMENT (of the abstract entered in Block 20, If different from Report)

JAN 2 0 1984

18. SUPPLEMENTARY NOTES

Proceedings of the Symposium on Turbulence, 8th Rolla, Missouri, University of Missouri 1984

19. KEY WORDS (Continue on reverse side if necessary and identify by block number)

FLUID MECHANICS
TURBULENCE
BOUNDARY LAYERS
COHERENT STRUCTURES
FLOW VISUALIZATION

20. ABSTRACT (Continue on reverse side if necessary and identify by block number)

A model of the near-wall behavior of turbulent boundary layers is presented. Based on an extensive series of primarily visualization experiments, which are described in overview, the model proposes a sequence of events which give rise to the bursting behavior responsible for turbulence production in the near-wall region. The model illustrates how hairpin vortex flow structures, generated during low-speed streak break down and ejection, are also responsible for the streak regeneration process, thus defining a clear cycle of turbulence generation for the near-wall region.

AFOSR-TR- 83-1336

A SYNTHESIZED MODEL OF THE NEAR-WALL
BEHAVIOR IN TURBULENT BOUNDARY LAYERS

C.R. Smith
Dept. of Mechanical Engineering &
   Mechanics
Lehigh University
Bethlehem, PA 18015

I. ABSTRACT

A model of the near-wall behavior of turbulent boundary layers is presented. Based on an extensive series of primarily visualization experiments, which are described in overview, the model proposes a sequence of events which give rise to the bursting behavior responsible for turbulence production in the near-wall region. The model illustrates how hairpin vortex flow structures, generated during low-speed streak break down and ejection, are also responsible for the streak regeneration process, thus defining a clear cycle of turbulence generation for the near-wall region.

II. INTRODUCTION

Over the past several decades it has become increasingly clear that the enigmatic behavior we refer to as turbulence has a systematic organization. Indeed, with each passing year more and more studies discover order (albeit complex order) among what was classically considered a totally irregular, chaotic flow behavior. For excellent reviews tracing this recognition of structured behavior in turbulent flows, the reader is referred to Willmarth (1975,1978), Kline (1978), and Cantwell (1981). However, despite the discovery of ordered and coherent structure in turbulence, researchers are still struggling to establish the rhyme and reason of the structures, and to describe the intricate processes of energy transfer and dissipation for which the observed structures are the vehicle.

Turbulence researchers are very much like archaeologists who seek the origin of man by extrapolative evaluation of bits and pieces of fossilized remains; we try to piece together experimental observations and the "remains" which our measurement techniques allow us to obtain with the hope that we can establish not only the size and shape of the turbulence "beast," but its modes of growth, death, reproduction, and interactions with other "beasts." Unfortunately, the bits and pieces of information we have for turbulent boundary layers still leave many holes in the morphological puzzle; consequently, current researchers still can't agree whether our "beast" is large or small, or whether we have more than one beast, or if (like the caterpiller/butterfly) we have a beast which passes through some metamorphosis. For detailed evaluations of the degree of agreement/disagreement on the various aspects of turbulent boundary layer flow structure the reader is referred to several collective position papers [Smith & Abbott 1978, Kline & Falco 1980, Brodkey & Wallace 1982].

What I wish to do in this paper is to recount some of the bits and pieces of "evidence" my colleagues and I have managed to uncover about the structure of boundary layer turbulence, and from this synthesize my present conception of the process of turbulence production, dissipation, and regeneration. The majority of my synthesized model will deal with the behavior in the near-wall of turbulent boundary layers ($y^+<100$), but it will at least peripherally address the development of the outer region.

01 19 099

-1-

Why address primarily the near-wall behavior and structure? There are three principal reasons. First, the boundary surface (hereafter referred to as the wall) is the sole source of all vorticity that comprises the boundary layer. On the average for a turbulent boundary layer, approximately 70% of this vorticity remains within $y^+<100$ of the wall (approximately 50% is within $y^+<20$). It seems quite logical that the vorticity dynamics in this confined region must strongly affect the development of the entire boundary layer, as well as the momentum exchange process at the wall, which results directly in the wall shear stress (not to mention heat and mass transfer). Second, the near-wall is the region of the most active turbulent fluctuations; all turbulence intensity components and Reynolds stresses reach their maximum values very near the wall. Again, the structure responsible for this most energetic region should be of key importance in the overall turbulence process. Third, repeated observations and measurements [Kline et al. 1967; Kim et al, 1971; Blackwelder & Kaplan 1976; Achia & Thompson, 1976; Lee et al, 1974; Oldaker & Tiederman, 1977; Smith, 1978; Blackwelder & Eckelmann, 1979; Kreplin & Eckelmann, 1979; Falco, 1981; Utami & Ueno, 1979; Nakagawa & Nezu, 1981; and Smith and Metzler 1983] have shown the near-wall region to be the source of the most universally organized and identifiable structure (i.e. low-speed wall streaks) and the most detectable event (i.e. the near-wall bursting behavior). No other region of a turbulent boundary layer displays flow structure characteristics so universally detectable or agreed upon as wall streaks and bursting. It stands to reason that the region in which the most repetitive flow structures or events occur must have a pronounced effect on the flow field as a whole (vortex shedding in the near-wake of a cylinder, or vortex coalescence in a mixing layer are supporting examples of this premise.) Taken collectively, the above three points appear to more than justify the close scrutiny of the near-wall region of boundary layer turbulence.

Because of its importance, the near-wall region has attracted a considerable amount of analytical and experimental attention. Numerous researchers have suggested various models of near-wall and wall region behavior, which draw on available research results together with varying degrees of interpretation and speculation. These models include large eddy interaction and Taylor-Gortler models [Nychas et al.,1973; Cantwell et al.,1977; Brown & Thomas,1977; Praturi & Brodkey, 1978], outer flow impact models [Falco,1978; Falco, 1981], counter-rotating streamwise vortex models [Bakewell & Lumley,1967; Blackwelder,1978; Blackwelder & Eckelmann, 1979], horse-shoe loop vortex models (outer scaling) (Theodorsen,1952; Willmarth & Tu, 1967; Nakagawa & Nezu, 1981], and hairpin loop vortex models (inner scaling) [Kline et al.,1967; Offen & Kline,1973, 1975; Hinze,1975; Smith,1978, Head and Bandyopadhay,1981; Perry et al.,1981; Wallace,1982; Perry & Chong,1982; Smith & Metzler,1983].

Expressing a personal bias, it appears that the hairpin vortex models have the most immediate and universal support, and can most clearly and logically explain the observed characteristics in the near-wall region. Hinze's hairpin vortex model provides the clearest scenario relating the known events and characteristics in the near-wall, while the review by Wallace provides the clearest argument and evidence for the predominance of hairpin vortices in the near-wall region. The detailed model by Perry and Chong (1982) presents an attractive hypothesis of how hairpin-type vortices of near-wall scale can interact to establish the behavior and structure of the entire boundary layer, providing the most promising potential link thus far between near-wall and outer-region behavior.

Although a hairpin vortex loop model appears conceptually promising, previous models have several deficiencies; the three most serious of these are: 1) Although hairpin vortices have been observed in one study to extend across essentially the entire boundary layer [Head & Bandyopadhay, 1981] and to occur in a quite organized fashion in transitional boundary layers [Perry et al.,1981], their presence in the near-wall of a fully turbulent boundary layer and their connection to the events there has not been conclusively demonstrated. 2) Despite the assumption that the stretched "legs" of the hairpin create the low-speed streaks

by concentration of low-speed fluid between them, it is unclear how this process can account for the apparent extreme length and persistence of the streaks [Oldaker & Tiederman,1977; Blackwelder & Eckelmann,1979; Smith & Metzler,1983]. 3) The bursting sequence has been described [Kim et al., 1971] to be the lift-up of a low-speed streak from the wall, followed by a violent oscillation and break-up of the lifted streak; if loops form in the near-wall, it is unclear what their role is in this bursting sequence. Offen & Kline (1975) speculate that a hairpin vortex forms just prior to streak oscillation; Hinze (1975) suggests that the hairpin vortex forms after the break-up of a streak, as a result of the inflow of fluid toward the wall to replace the ejected bursting fluid. Wallace (1982) suggests that local pressure field fluctuations distort and destabilize shear layers diffusing from the wall causing hairpin vortices to form, which by their interactions perpetuate the local pressure fluctuations; however, Wallace does not clearly suggest the role of the hairpin vortices in the near-wall or how the evolution of the vortices is tied to the bursting process, or streak formation. Head & Bandyopadhay (1981) and Perry and Chong (1982) discuss the formation of hairpins as necessary for development of turbulent boundary layers, but do not tie them to any particular structure or event other than to suggest they form from sublayer material and are related in scale to the mean spacing ($\lambda^+ \dot= 100$) of the low-speed streaks.

In addition to the above deficiencies in previous hairpin vortex models, two general deficiencies shared by all current models of near-wall behavior are: 1) Despite the concensus that bursting of the low-speed streak does occur, it is quite unclear what mechanism causes the burst fluid to move rapidly outward. Suggested mechanisms include interaction with vortices resulting from previous upstream bursts [Offen & Kline,1975], vortex loop induction effects [Willmarth & Tu, 1967; Hinze 1975] and "pushing" of fluid away from the surface due to continuity by an outer region sweep [Brodkey,1978]. 2) While it is apparent that a cyclic process of turbulence production in the near-wall does take place [Kim et al, 1971;

Hinze,1975; Offen & Kline,1975], the structural characteristics and dynamic processes of this cycle have not been well defined (not to mention the extent to which this cyclic process involves the outer region). Generally, most suggested cyclical processes are not cycles, but monotonic sequences of kinematic events which either do not clearly define the "loop" in the cycle, or depend on the existence of certain structures which are critical to the postulated process but whose source is of undetermined origin [e.g. counter-rotating streamwise vortices (Blackwelder,1978), pockets (Falco ,1978, 1981), hairpin vortices (Perry & Chong,1982); and sweeps (Praturi & Brodkey,1978)].

This enumeration of the deficiencies of previous near-wall and wall region turbulence models now brings me to the objective of the present paper: to propose a more comprehensive model of the near-wall behavior in turbulent boundary layers. The model to be proposed is based primarily on a series of diverse experimental studies of turbulent boundary layers performed by myself and my colleagues at Lehigh University, although the previous work and ideas from many of the other studies cited in this paper clearly initiated and motivated our thinking, and guided our selection of experimental configurations. The studies to be cited are primarily visualization studies, supported to varying degrees by probe and statistical measurements. I imagine my emphasis on flow visualization will be criticized by some, but it has become clear to me over the past several years that we have no chance either of making appropriate probe measurements of a behavior or of analytically modeling that behavior unless we can establish quite clearly what the behavior we are seeking is. And it is my contention that our only recourse for identifying that behavior is via carefully planned visualization studies such as I will discuss here.

My approach in the remainder of this paper will be to briefly describe the system on which our studies were conducted and then to provide a brief overview of each study, its objective, and what was learned as it pertains to near-wall behavior. The research overviews will be presented in two sections: 1) Turbulent structure studies and 2) discrete hairpin vortex studies. In the former, the

focus was on visualization of the behavior of fully turbulent boundary layers; in the latter studies, the behavior and dynamics of experimentally generated hairpin vortices were examined to allow cross-comparison with the fully turbulent behavior. Each section is subdivided according to each different viewing perspective or combination of views, with these subdivisions arranged to systematically illustrate the characteristics of the near-wall flow structure. Based on these studies, a synthesized model of what is speculated to be occurring in the near-wall region will be developed and discussed.

III. GENERAL EXPERIMENTAL SYSTEM

The series of studies cited in this paper were all performed in a free-surface water channel facility with a 6m working section, 0.9m wide by 0.3m deep as described in Smith & Metzler (1983). A general schematic of the cross-section of the working section with associated equipment is shown in Figure 1.

Visualization of the flow structure and behavior was done using a variety of specially designed hydrogen bubble-wire probes which allow a 25mm dia. platinum wire to be oriented either transverse or normal to the flow direction. The hydrogen bubble-lines are generated using a specially designed generator unit, built in our laboratory. Using the probes and generator, lines and sheets of hydrogen bubbles can be introduced either parallel or normal to a test surface at any desired height and frequency.

The viewing and recording system employed in the studies is a two-camera, high-speed video system (manufactured by the Video Logic Co.) which incorporates synchronized strobe lights to provide 120 frame/s with effective frame exposure times of 10^{-4}s. A split-screen capability allows two different fields of view to be simultaneously displayed and recorded. All recorded data can be played in flicker-free slow motion (both forward and reverse), as well as single-framed for detailed data analysis and hard copy output. For some studies, a specially designed fiber optic lens, 1 cm in diameter and 1 m long, was incorpor-

ated with one of the video cameras to yield end-on views of the hydrogen bubble-wire [see Smith & Schwartz, 1983].

Once a video sequence is recorded, conventional still photographs of individual stop-action frames, such as appear in this paper, can be taken directly from the video screen.

IV. RESEARCH OVERVIEW: TURBULENT BOUNDARY LAYER STRUCTURE STUDIES

A. Top-View Studies

Using a bubble-wire oriented transverse to the flow direction (figure 1), top-view sequences of the flow behavior in the region $1<y^+<40$ were obtained and the detailed characteristics of the low-speed streak structures which dominate the very near-wall region of turbulent boundary layers were examined for a Reynolds number range of $740 \leq Re_\theta \leq 5830$ [Smith & Metzler, 1983]. The low speed streak pattern, as illustrated in Figure 2, was found to be essentially identical in appearance and character for all Reynolds numbers examined. Using visual counting techniques for extended video sequences, the statistics of non-dimensional spanwise spacing of the low-speed streaks were determined and shown to be essentially invariant with Reynolds number, exhibiting consistent values of mean non-dimensional spanwise spacing ($\bar{\lambda}^+ = \lambda u_\tau/\nu \approx 100$) and remarkably similar probability distributions conforming to lognormal behavior. Further studies showed that streak spacing increases with distance from the wall due to a merging and intermittency process which occurs for $y^+ \gtrsim 5$. An additional observation was that although low-speed streaks are not fixed in time and space, they demonstrate a tremendous persistence, often maintaining their integrity and reinforcing themselves for time periods up to an order of magnitude longer than the observed bursting times associated with wall region turbulence production. This persistence behavior is illustrated quite clearly by Figure 3 [from Smith and Metzler, 1983], which indicates the temporal persistence of streaks as identified using a systematic visual counting technique.

A further investigation of streak persistence and longevity was carried out through an experiment

which capitalized upon the observation that stray particulate matter on the channel bottom appeared to resolve itself into long streamwise aggregations. This study [Metzler, 1981] involved the injection of a thin slurry of 100 μm glass beads (e.g. ≈ 2 and $d^+ = 1$) along the surface beneath a fully turbulent boundary layer. Within a few seconds after injection the beads collected into streamwise concentrations of width $\Delta z^+ \approx 35$ which extended essentially uninterrupted the length of the channel with a nearly uniform spanwise spacing of $\Delta z^+ \approx 80$. This pattern appeared stable and quasi-stationary, with the only movement being a quasi-periodic buffeting and a gradual downstream migration of the beads, apparently in response to localized velocity fluctuations. Further investigation with a horizontal hydrogen bubble-wire disclosed that the bead concentrations essentially coincided with the low-speed streaks, as shown by Figure 4.

Since the beads used were not light enough to move freely with small velocity fluctuations, the results of this experiment should be interpreted with some caution. While it is possible that the bead concentrations tended to mark the "mean" locations of very long, naturally occurring low-speed streaks, it is more probable that the wakes induced by the streamwise aggregations of the beads acted to cause their further concentration downstream. However, since the hydrogen bubble flow patterns occurring directly above the lengthy, coherent bead concentrations were those of low-speed streaks, this implies that the flow structures forming above the beads (and causing their continued concentration) must be the same structures which occur naturally, only more focussed by the presence of the beads.

The apparent stabilization of the lateral location of low-speed streaks by the agglomerations of glass beads suggested that spanwise surface perturbations elongated in the streamwise direction could potentially function as "formation sites" for development of the low-speed streaks. To carefully examine this suggestion a study was done employing a combination of hydrogen bubble-wire flow visualization and hot-film anemometry measurements to examine the effects of sublayer

scale streamwise surface modifications on near-wall flow structure [Johansen and Smith, 1983]. Using monofilament fishline of an approximate nondimensional height of $h^+ = 4$, the effects of nondimensional spanwise line spacings for $60 < S^+ < 160$ were examined. The results indicate that the lines appear to act as nucleation sites for low-speed streaks, as shown in Figure 5. Statistical evaluation of streak stabilization effects indicated that the presence of the lines had the greatest effect for $S^+ < 100$, but that for $y^+ > 10$ the stabilizing effect of the lines on streak behavior diminished for all line spacings examined, with the near-wall behavior relaxing back toward that characteristic of an unmodified surface. The confinement of the effect of the lines to the very near-wall region was borne out by measured mean velocity and turbulence intensity profiles, which indicated discernable variations from unmodified flat plate behavior only for $y^+ < 30$. In essence, sublayer surface modifications appear to influence turbulent structure behavior only in the very near-wall region, indicating that despite the forced organization of the low-speed streak regions adjacent to the wall, this organized effect is lost quite rapidly a short distance above the wall.

B. Split-Screen Studies: Top-End Views

The bead concentration studies suggested that some streamwise mechanism which occurs in a repetitive fashion must be responsible both for the extreme streamwise length of the bead concentrations and for the formation of low-speed streaks. In an attempt to reveal both the presence and the characteristics of the streamwise behavior, a dual-view study [Smith and Schwartz, 1983; Schwartz, 1981] was conducted using a fiber-optic lens to obtain simultaneous top-end views of the near-wall region within which low-speed streaks are observed. A schematic of the physical configuration is illustrated in Figure 6.

Figures 7 and 8 show two typical dual (top-end) view sequences of the streak behavior taken for $Re_\theta = 1700$. The two sequences, both taken with the bubble-wire at $y^+ = 14$, are to the same scale and correspond to conventional orthographic projections (i.e., the lower picture is the end-view

projection of the corresponding top-view above). The flow is top to bottom in the top-views and out of the picture in the end-views; the bubble-wire appears at the upper extreme in the top-view and about mid-picture in the end-view. The two dark rectangles appearing near the top of each picture are scene and frame indicators inserted electronically by the video system.

It was found that bubble-lines generated in close proximity to each other tended to obscure one another when viewed in end-view. Thus, the sequences presented here employ single-realization time-lines in order to clarify the local flow dynamics. For the end-view pictures, the fiber optic lens was located 12 cm downstream of the wire at a viewing angle of about 2° to the surface. Thus, the bubble lines in the end-views will appear to move slightly downward as they progress towards the lens. In addition, the lighting and lens aperture limited the end-view depth of field to about 3 cm. So the bubbles nearer the lens frequently appear defocussed.

The top-view in Figure 7a illustrates the very strong spanwise velocity variations that exist in the wall region, with the corresponding end-view sequence showing the strong vertical movement and the extreme spanwise discreteness of the low-speed regions (which correspond to the low-speed streaks illustrated by Figure 2). Close examination of the end-view of Figure 7b reveals the beginning of a "mushrooming" effect for each of the low-speed regions. This indicated a spreading of the low-speed fluid in a spanwise direction as it moves upward. Notice that the low-speed upwelling on the far left has developed a definite "hook" in the bubble-line which was observed to be the result of a strong streamwise vortex adjacent to the line.

In the top-view of Figure 8a, discrete low-speed regions (two appear in this sequence) again appear as the dominant characteristic. The corresponding end-view again shows these to be well-defined upwellings of fluid. In the following picture, the bubble-line has passed out of the top-view, but in the end-view the low-speed upwelling on the right has developed from a double-hook appearance in Figure 8a into a double-loop in Figure 8b (this pattern was also observed for the

left upwelling, but it is not as clearly shown by the still photographs). Repeated observation of these mushroom and double-loop patterns revealed quite clearly that they are the resultant patterns created by a pair of counter-rotating streamwise vortical structures in proximity to the wall.

Detailed examination of a series of dual-view sequences over a wide range of Reynolds numbers and y^+ values has shown the low-speed streaks to always be regions of vertical motion, with the bubble line patterns frequently revealing associated streamwise rotation (40% of observations) or counter-rotating vortex pairs (15-20% of observations). Evaluation of the characteristics of the vortical motions indicate that they are fairly substantial in extent and strength, with streamwise vortices observed to occur over a range in dimensionless diameters from $10 < D u_\tau / \nu < 40$ and mean vorticities from $0.05 < \omega_x \nu / u_\tau^2 < 0.6$ in the near-wall region. Generally, the degree and characteristics of observed counter-rotating vortices varied with wire location from the wall [Schwartz, 1981], with $y^+ = 25$ indicated as the most probable location for detecting a vortex center. In addition, the apparent diameter and strength of the observed streamwise vortices were generally larger the farther from the wall the vortices were detected.

Probably the most important observation from this dual-view study was that whenever counter-rotating vortices were detected in end-view, they were always observed in the corresponding top-view to evolve either from or in conjunction with a pattern indicating a low-speed streak. Thus, it was apparent that the presence of counter-rotating, streamwise vortices is either necessary for or the result of low-speed streak formation. This latter point is confirmative of the flow structure symbiosis suggested previously by Lee et al. (1974), Blackwelder (1978), and Blackwelder and Ecklemann (1979).

C. Split-Screen Studies: Top-Side Views

In order to further examine the three-dimensional aspects of the near-wall flow behavior, and to hopefully establish the origin of the counter-rotating vortices which top-end view studies indicated to be intimately involved in low-

speed streak formation, a series of studies was done [Metzler,1981] employing simultaneous side and top-views of a horizontal hydrogen bubble-wire. The general viewing orientation is shown schematically in Figure 9. A slightly oblique positioning of the side-view camera at a small downwards angle (7°-9°) yielded an improved perspective of the horizontal bubble wire over that which would be obtained if the line-of-sight was parallel to the wire. The cameras were carefully adjusted to obtain equal magnification scales and coincident streamwise fields-of-view.

A problem that inevitably accompanies use of split-screen viewing is the difficulty in identifying the same spanwise location in both the side and top-views. In the present study, this problem was overcome by insulating all but a one-centimeter span of the bubble-wire, thus producing a narrow bubble sheet that is entirely within the viewing depth-of-field. For the flows examined, the width of this bubble sheet was of the order of one streak spacing ($\Delta z^+ \doteq 110$). This approach permits (1) a direct association to be made between the top and side-views, and (2) all bubble-lines produced to be kept in focus.

Basically, several different types of flow structure were observed to occur in the near-wall region. The most dominant was the narrow, well defined low-speed streak, which was always observed to be a region of upwelling motion. Depending on the position of the wire, these low-speed streaks often were observed to undergo a strong transverse movement (in top-view), causing the streak to become "kinked" or wavy as shown in Figure 10a. Alternatively, the streak would be observed to degenerate into one or more spanwise bulges (almost a bisymmetric "kink") as shown in Figure 10b. These bulges appear to be the "pockets" described in previous studies by Falco (1978, 1981) and Smith (1978). In both cases, a series of vertical undulations in the streak could frequently be observed in side view to form transverse and sometimes streamwise rotational motions. The formation of these undulations and the breakdown into rotational elements appears to be what Kim et al. (1971) originally described as the streak oscillation and break-up portion of the "bursting"

sequence in the near-wall region.

Less frequently, streaks were observed to break down in a more symmetrical fashion into an apparent series of 2-5 hairpin-like vortex structures. This was normally due to a fortuitous coincidence of wire location and the position and phase of the streak bursting, but was observed with bubble-wire locations in a range of $5 < y^+ < 35$. Figure 11 is a sequence showing the evolution of one such a vortex structure (marked HP on the Figure) from such a series. The remnants of the legs of previously generated hairpin vortices can be observed in this figure (although they are difficult to identify in these still pictures). Figure 12 is a schematic representation from Smith & Metzler (1982) of this type of combined hairpin vortex flow structure with associated characteristics. Note that the vorticity associated with the upstream-pointing legs of the vortices is oriented similarly to that of the counter-rotating vortices discussed earlier in conjunction with streak formation. Note also the suggestion of a coalescence of these legs from multiple, nested hairpin vortices as a mechanism or reinforcement of the streamwise, near-wall vortices.

Employing a series of video sequences, the convection characteristics of identifiable hairpin vortices were evaluated. It was generally determined that the trajectories of individual hairpin "heads" typically did not evolve and demonstrate a substantial upwards component below a height of $y^+ \doteq 15$. A limited study indicated that a vortex head which was detected at $y^+ = 15$ would (on the average) move outward, reaching a height of $y^+ = 80$ after traveling a distance of $\Delta x^+ = 350$ downstream. At $y^+ \doteq 40$, the average streamwise convection velocity was determined to be $U_c = 13.1 \, u_\tau$, and the upwards normal component was $v = 2.2 \, u_\tau$. The former value (U_c) is close to the convection velocity associated with the ejection phase of the bursting cycle as measured by Kline et al. (1967), i.e. 13.8 u_τ at $y^+ \doteq 40$. Where discrete arrays of typically 2-5 hairpin like ejections could be observed, the mean spacing between the heads was typically $\Delta x^+ \doteq 200$ to 150. Separate arrays of hairpins, kinks, or bulges were observed to appear at time intervals between the arrays commensurate with the empirical expressions for the bursting

-7-

frequency based on inner variables ($f^+=fv/u^2=.005$), or outer variables ($U_\infty T_B/\delta=5$), which are nearly coincident for the moderate Reynolds numbers examined in this study.

In addition to the apparent formation of an array of hairpin-like ejections during the "bursting" of a streak, it was observed that a given streak will frequently persist and give rise to multiple bursts. In numerous cases a low-speed streak was observed to persist for times as long as $4-5T_B$, resulting in the generation of several loop arrays. In essence this observation is consistent with the observations of the previous streak persistence study described in Section IV.A, and implies that the formation of the hairpin vortex arrays may be the mechanism causing both the low-speed streak formation — perpetuation and the great streamwise length of the bead concentrations.

D. Side-View Studies

To this point, only studies employing a horizontal, spanwise oriented bubble-wire have been described. Clearly this tends to emphasize the local aspects of near-wall behavior while leaving us somewhat ignorant of the characteristic changes in behavior with distance from the wall. To examine those changes, a series of side-view studies of a vertically oriented hydrogen bubble-wire were done. Two examples of such a side-view which encompass a vertical region of about 3/4 the boundary layer thickness are shown in Figure 13, illustrating a number of the characteristics of the flow structure as it appears in side-view.

Note that the interior of the boundary layer appears to consist of a complicated agglomeration of vortical structures (or patterns) of much smaller scale than the boundary layer thickness. Closer examination indicates that these patterns appear to increase with distance from the surface, achieving an order of magnitude of $\Delta\ell^+=100$ toward the outer region of the boundary layer. Additionally, as these smaller patterns move outward from the surface, they are observed to apparently gather into large, less active motions, moving in weakly circulatory patterns. In essence, the observations of this outer region are in general agreement with the previous outer region smoke

visualization of Falco (1977, 1981), Nagib et al. (1978), and Head and Bandyopadhay (1981). However, whereas smoke injection techniques tend to illustrate the cumulative characteristics of the flow since introduction of the smoke, the introduction of the hydrogen bubbles immediately adjacent to the region of interest illustrates the local, active motions in the flow. Although it cannot be shown in the still pictures presented here, repeated slow motion viewing of the original video sequences indicates that the outer region appears to grow by the agglomeration of smaller scale motions (which appear to have their origin in the wall region) into the larger scale outer region motions through some complicated process of vortex coalescence. This coalescence and growth of smaller scale structures near the surface into larger scale vortical flow structures toward the outer region is consistent with the previous suggestions of Offen and Kline (1975) and Perry and Chong (1982), and of course satisfies the linear growth in scales which is a primary assumption giving rise to the log law velocity profile in the wall region.

A further general aspect of the boundary layer flow structure, particularly near the wall, is the appearance of a series of structures "linked" together in some complicated fashion. These structures frequently appear as a combination of several structures of predominantly spanwise rotation linked by structures of essentially streamwise rotation. These combined structures are generally observed to project downstream and away from the wall at angles of 15° to 40° (depending on the distance from the surface). In some instances these linked structures could be traced from the near-wall to well into the outer region. Both pictures in Figure 13 illustrate the "linked" behavior quite clearly, with figure 13a a particularly good example.

E. Split Screen Studies: Side-Side Views

To provide a much more detailed view of the near-wall flow behavior in side-view, a unique split-screen procedure was employed, as shown in the two picture sequence of Figure 14. This technique employs one camera to view and record a wider view of the general boundary layer behavior

and a second camera to view the near-wall region exclusively. In Figure 14, the general view appears as the upper picture, with the simultaneous view of the near-wall region superposed as the lower picture, comprising approximately the lower 40% of the general view. Note in the near-wall pictures that the small streamwise irregularity in the bubble-lines (labeled "I" in Figure 14a) is the wake of a 12 μm diameter fiber stretched spanwise across the flow to provide the lower probe support for the vertical hydrogen bubble wire; the support is less than 1 viscous length in diameter and introduced no irregularity into the flow pattern other than the streakline wake.

The pattern illustrated in the near-wall picture of Figure 14a is very commonly observed in the near-wall, and is a clear example of the "linked" vortical flow structure described above, with the bubble-line pattern depicting connected spanwise and streamwise vortical structures inclined at an angle of about 16° to the wall. The combined structure has an undulating and wave-like appearance with a continuation of this undulating and linked behavior detectable in the upper, general view picture. Figure 14b is a picture taken $t^+ = \Delta t \, u_\tau^2/\nu = 22$ earlier than Figure 14a, illustrating the preceding portion of the "linked" structure which projected even farther out from the surface with the same characteristic, undulating behavior. The structure into which the coherent vortical head observed in Figure 14b evolves is indicated by the intersection of the arrows in Figure 14a. Clearly the coherency of the structure is lost to the observer as the structure 1) interacts with other structures and 2) moves farther from the source of introduction of the visualization material.

The type of "linked" vortical pattern illustrated by Figure 14 was generally observed as a consequence of the lift-up and oscillation of a low-speed streak during the bursting process. Generally, the development of such a pattern was preceded by the appearance of a strong inflectional profile, followed by the development of a streamwise waviness, and subsequent shear layer break down. However, this "break down" process was observed to retain a remarkable degree of coherence

and organization in that rather discrete vortical patterns in both the spanwise and streamwise direction would rapidly develop, followed by their rapid movement upward away from the surface and out of the near-wall. As these "linked" patterns moved away from the wall, one of two general fates befell them; when traced into the general view, the linked structures would either 1) interact with existing vortical structures in the outer region, losing their original near-wall organization, or 2) (less frequently) maintain their "linked" appearance, projecting further into the boundary layer until they passed from the field of view.

Clearly, the process described in the previous paragraph and shown in Figure 14 is a bit idealized, and very dependent on the proper juxtaposition of the low-speed lift-up with the hydrogen bubble-wire. However, whenever a lift-up occurred in the field-of-view, the development of linked vortical elements which propagated away from the surface in an organized manner could be observed either in total or at least in part. In essence we appeared to see essentially the same near-wall behavior as detailed in Kim et al. (1971) and Offen and Kline (1975), however the combination of a higher Reynolds number and access to much more extensive visualization footage allowed us to see more of the details of the bursting process than those two studies.

The linked vortical elements observed to form as an apparent result of the bursting process are essentially the same formation described in the split screen top-side views of the previous section as a series of hairpin vortices. Generally, the initial origin of the linked vortical structures occurred in the region $10<y^+<30$, with the spanwise spacing between elements of approximately $\Delta x^+ \simeq 150$ to 200. These latter values are essentially consistent with the observed location and spacing of the apparent hairpin vortices observed in the top-side views.

V.   RESEARCH OVERVIEW: HAIRPIN VORTEX GENERATION STUDIES

Clearly there is the suggestion in this and many previous studies that hairpin vortices of

-9-

near-wall scale are an integral part of the tur-
bulence generation process in the near-wall.
Figure 12 suggests how such vortices are collec-
tively oriented to yield the observed bubble pat-
terns and Figure 14 appears to display the span-
wise and streamwise elements of such a vortex. And
the dominance of hairpin type vortices are the
premise upon which both Head and Bandyopadhay (1981)
and Perry and Chong (1982) build their models of
the turbulent boundary layer. However, the pres-
ence or absence of hairpin vortices generally rests
on a subjective pattern recognition process based
on the visualization patterns that each observer
expects a hairpin vortex will yield with a parti-
cular visualization technique (note that the same
point frequently applies to pattern recognition of
sensor generated signals as well). In the case of
hydrogen bubble-wire visualization, the very capa-
bility of the medium to visualize localized behav-
ior is what makes it difficult to interpret bubble-
line patterns resulting from the influence of only
parts of three-dimensional flow structures such
as hairpin vortices. Since we cannot visualize
the entire flow field created by a hairpin vortex,
one potential way to detect the presence or absence
of hairpin vortices in the near-wall is to estab-
lish the types of patterns which such flow struc-
tures yield, categorizing them in terms of both
the phase of development of the flow structure
and the relative location of the marking wire.
From this information one then has the basis for
making rational visual pattern identifications of
the presence of hairpin vortices.

This second research overview 1) describes
a technique we have employed to establish the
patterns which characterize hairpin vortices and
2) demonstrates the similarity between several of
these patterns and those recurrent patterns
observed in the near-wall of turbulent boundary
layers.

A. Hairpin Vortex Generation

Through a process of experimental serendipity
it was determined that hairpin vortices can be gener-
ated by the interaction of a hemispherical protu-
berance with a subcritical, developing laminar
boundary layer. Under the proper conditions, a

hemisphere will shed hairpin vortices extremely
periodically and with very repeatable characteris-
tics, as illustrated schematically by Figure 15.
In Figure 16 the head of a hairpin vortex loop as
it initially develops in the wake of a hemisphere
is revealed by hydrogen bubble time-lines generated
with a wire oriented vertically in front of the
hemisphere.

Using dye and hydrogen bubble-wire visualiza-
tion in conjunction with hot-film anemometry mea-
surements, the characteristics of the hairpin vor-
tices have been examined over a wide range of par-
ameters [Acarlar and Smith 1984]. The extensive
visual studies indicate that the loop formation
and interaction process is very complicated and
three-dimensional, developing many convoluted, ye'
very repeatable patterns as the hairpin vortices
convect downstream. As will be illustrated below,
the type of visual pattern observed is very depen-
dent upon the location and orientation of the
bubble-wire.

B. Combined Top-Side Views

Although many, many different visualizations
of the bubble-line patterns created by hairpin
vortex structures have been done, probably the
most revealing study is that done using simultan-
eous top and side-views of a horizontal hydrogen
bubble-wire. Essentially, this is the same view-
ing technique employed for the dual-view turbulence
studies shown in Section IV.C above. By placing
the bubble-wire at different locations downstream
of the hemisphere and at different heights above
the surface, the local behavior of the flow in
response to the presence and passage of the hair-
pin vortices can be observed. Figure 17 shows
three examples of the different types dual-view
bubble-line patterns obtained with the bubble-wire
located five radii downstram of the hemisphere and
at three different heights relative to the wall.

The dependency of the observed bubble-line
patterns on the relative location of the bubble-
wire within or in proximity to a hairpin vortex is
clearly illustrated by Figure 17. It is safe to
say that without access to both the top and side-
views in these pictures, it is difficult, if not
impossible, to properly interpret the complete

-10-

local fluid motion. One only need study Figure 17c for a few seconds to realize how improbable it would be to properly infer the flow pattern (and thus the fluid motion) in one view from the other. The ramifications of these pictures on the potential existence of similar hairpin vortex structures in turbulence can best be illustrated by comparing the patterns of Figure 17 with the patterns obtained using a similar visualization configuration in the near-wall of a turbulent boundary layer, as shown previously in Figures 10 and 11. Although we cannot expect a one-to-one correspondence of patterns since hairpin structures in the near-wall region will vary in their degree of symmetry, virtual origin, and degree of amalgamation with each other, there does appear to be a remarkable degree of similarity between the turbulence patterns and various "pieces" of the hairpin vortex patterns (compare particularly Figures 17b and 17c with Figures 10b and 11). A further remarkable similarity can also be seen between the top-view of Figure 17c, obtained near the surface beneath a hairpin vortex structure, and Figure 2 which illustrates the classic low-speed streak pattern in the very near-wall region.

C. Side and Top-Views

To further emphasize the similarity between the hairpin vortex bubble-line patterns and those observed in the near-wall region, Figures 18, 19 and 20 are shown. Figure 18a is a side-view picture of a hairpin vortex pattern obtained with a vertical bubble-wire 20 radii downstream from the generating hemisphere. Figure 18b is a dual side-view (similar to Figure 14) of a turbulent boundary layer. Comparison of the vortical pattern of Figure 18a with the essentially identical patterns shown in the near-wall region (bottom view) of Figure 18b and Figure 14 appears to leave little question that the bubble-line patterns are created by essentially the same flow structure.

Figures 19a and 20a are top-view bubble-line patterns created by a hairpin vortex passing over a horizontal bubble-wire again 20 radii downstream of the hemisphere. These pictures are compared in Figure 19b and 20b with bubble-line patterns obtained in the same manner in the near-wall of

a turbulent boundary layer (but not in same scale). The similarity between these two sets of pictures is striking. The similarity is so striking in the actual video footage that one can draw no other conclusion than the same type of flow structure, or some variation of it, is the source of all these patterns.

VI. MODEL SYNTHESIS

The overviews presented above strongly suggest that hairpin vortices are quite pervasive flow structures in the near-wall region, leaving their "footprints" in the bubble-line patterns in all regions of the near-wall. This is not an unexpected finding since the work of Head and Bandyopadhay (1981) suggests that such vortex structures appear to be a mainstay of the observed flow structure in the outer region as well. And as pointed out in Section II, the hypothesis of hairpin or horseshoe-type vortices playing a major role in turbulent boundary layer behavior has found widespread support among a number of researchers.

The studies reviewed above in Sections IV and V illustrate not only the presence of hairpin-type flow structures, but also indicate some of their characteristics. Among these is the observation that they appear to occur in groups of two or more (Sections IV. C, IV. E) with a fairly consistent streamwise spacing. This observation suggests the presence of an amplified instability of some nature which promotes the three-dimensional roll-up and concentration of vorticity in a reasonably periodic fashion. The form of instability most generally suggested is that arising from an inflection in the local velocity profile. Such a profile has been observed or detected to form just prior to near-wall busting by Kim et al. (1971) using visual techniques, by Blackwelder and Kaplan (1976) using a hot-wire probe rake, and by Moin and Kim (1982), using a numerical, large eddy simulation technique. The occurrence of groups or packets of hairpin vortices at time intervals consistent with previously accepted bursting times (Section IV. C) suggests that the hairpin vortices are generated as a consequence of the inflectional instability.

Kim et al. (1971), in their seminal work on

wall region bursting behavior, show picture sequences obtained using hydrogen bubble visualization which indicate the development of what appear to be both longitudinal and transverse vortex structures following the appearance of an inflection in the near-wall velocity profile. Kim suggested that these vortex structures may have been parts of a lifted and stretched vortex loop (i.e. hairpin vortex) associated with the break down of the inflectional instability. Figure 21 is shown to suggest that Kim was correct, and that a near-wall inflectional instability does give rise directly to hairpin vortex generation. Figure 21 is a near-wall sequence taken with a vertical bubble-wire which illustrates a strong inflection in the vertical velocity profile (Fig. 21a) that breaks down rapidly (Figs. 21b, 21c) to form what appears to be the bubble-line pattern of a hairpin vortex (Fig. 21d, 21e). Comparison of Figures 21d and 21e with the experimentally created hairpin vortex bubble-line pattern in Figure 18a indicates a remarkable similarity, particularly with regard to the appearance of the legs of the vortices. Note that the head of the hairpin vortex is not as clearly shown by the still pictures of Figure 21 due to the head developing slightly out of the plane of the bubble sheet. However, the transverse rotation of the head could be clearly detected in the video sequence; the deformation near the top of the vortex legs in Figures 21d and 21e also shows the effect of the head on the bubble-line pattern.

The formation of one or more hairpin vortices during the break down of an inflectional instability is hypothesized as the mechanism which is construed as the streak bursting event in the near-wall. A schematic of the sequencing of this process is shown in Figure 22 for a burst event which generates three hairpin vortices. This model is developed primarily on the basis of our studies, but as will be discussed appears consistent with many previous observations. It should also be borne in mind that this Figure is a model of the process, which is illustrated to be a) symmetric, b) very coherent, and c) in isolation from similar events going on simultaneously around it. The real event will be none of the above, but for purposes of presentation and explanation the model is

shown in this idealized condition.

The model begins by consideration of a low-speed streak region since it is clear from previous studies and our present studies that the bursting event must be initiated from these low-momentum streak regions. Prior to a burst event, the streak region grows in extent (primarily in the normal and streamwise directions) by continued accumulation of low-momentum fluid (the process is explained below). The streak grows until the passage of a disturbance of sufficient size and strength impresses a local adverse pressure gradient (as suggested by Offen and Kline 1975) upon a portion of the streak region, causing a local deceleration of the near-wall flow. This local deceleration (caused most probably by the passage of a vorticity concentration created upstream) will have the greatest effect on the low-momentum streak region, creating a three-dimensional inflectional profile at the interface between the streak and the higher speed wall-region fluid. The extent of this inflection will generally depend on the magnitude of the local pressure disturbance and the extent of development of the streak. Once an inflection develops, the streak will be unstable to small local disturbances, of which the background turbulence in the outer region provides a rich supply. Depending on the size of the streak region and the extent of the velocity inflection, a three-dimensional oscillation will develop over the inflectional region, as shown orthographically in Figure 22a.

The oscillation of the streak introduces three-dimensional perturbations in the vorticity sheet which encompasses the low-momentum streak region. As Rosenhead (1932) points out, if viscous damping is small enough, these perturbations in the vorticity sheet will grow by a process of three-dimensional concentration of vorticity, effecting a vortex roll-up over the top and sides of the streak as shown in Figure 22b. The number of vorticity concentrations ("waves") developing over the inflected region will vary with the magnitude and extent of both the streak and the initial external disturbance, but will generally be 2 to 5, with observable vortex concentrations generally developing in the region $15 < y^+ < 30$.

As the vortex concentrations roll-up into

three-dimensional vortices, they take on the characteristic Ω (i.e. hairpin) shape as indicated in Figure 22c. Note that the Ω shape is created by the rotational vortex formed from a sheet of vortex lines which initially encompassed the top and sides of the streak; however, since the spanwise vortex lines comprising the initial vortex sheet must be contiguous, the lines which concentrate over and around the streak must turn and appear to the lateral sides of the streak region as the original sheet of vorticity, as shown schematically in Figure 22c.

Once the vortex concentrations begin to distort three-dimensionally, Biot-Savart interactions between the various portions of the vortex amplify the distortion of the vortex and create a self-induced movement of the hairpin away from the wall. This self-induced motion is caused by the stretching of the vortex in the streamwise direction (as a result of the steep velocity gradient near the wall), which creates a pair of counter-rotating legs with streamwise orientation. Mutual induction effect cause the forward portion of these legs and the head of the vortex to move away from the wall as indicated in Figure 22c. Since the trailing portion of the legs must connect back to the lateral vorticity sheets flanking the streak region, the trailing portions of the legs undergo extreme stretching by the velocity gradient, yet remain in close proximity to the surface. Since these trailing legs remain near the surface and develop strongly amplified vorticity concentrations as a result of the stretching process, they will 1) interact strongly with the wall and the sublayer fluid resulting in elevated viscous dissipation and 2) create a lateral pressure gradient which causes the further accumulation and concentration of low-momentum fluid between the legs of the hairpin vortex as per the mechanism suggested by Doligalski and Walker (1978). This latter effect provides the mechanism to both 1) pump low-momentum fluid away from the surface during the burst and 2) redevelop and perpetuate the low-momentum streak region following the burst event.

In addition to the lateral pressure gradient caused by the stretched legs, the heads of the hairpin vortices will create local streamwise pressure gradients which will result in a rapid lift-up d entrainment or ejection of low-momentum fluid from the low-speed streak as the head of a hairpin vortex convects downstream over the low-speed streak. This process is indicated schematically in Figures 22c and 22d, and can be observed developing in the bubble-line pattern of Figures 21c, 21d and 21e. Note that this rapid ejection of fluid by the passage of a hairpin appears consistent with the kinematic description of an ejection by Corino and Brodkey (1969). In fact, if one compares Figures 21d and 21e of this paper with Figure 6 of Corino and Brodkey, there is a striking similarity, with the indication of a high speed "sweep" following in close proximity to a vortex induced ejection (see Figure 21e).

As the burst event proceeds, the hairpin vortices continue to be stretched by the mean strain field with the head and upper portion of the hairpins moving farther away from the wall into regions of lower velocity gradients. If the outer portions of the hairpins do not interact with other surrounding or previously generated vortex structures (the most probable behavior), the head of the vortex will begin to diffuse and distort even further by Biot-Savart effects as shown in Figure 22d. This distortion of the head is shown nicely by Danberg (1978) in an inviscid numerical study of hairpin type vortices. As Figure 22d further illustrates, the subsequent hairpin vortices generated by the burst will also rise away from the surface such that the heads of the vortices roughly align themselves along an angle of 15° to 30° to the wall, with the angle appearing shallower in the near-wall and increasing as the vortices move farther from the wall. It should be noted that angles of 15° to 30° have been noted in several investigations [e.g. Brown and Thomas, 1977; Head and Bandyopadhay, 1981] as the range of angles over which inclined turbulent "fronts" have been detected by probe measurements within turbulent boundary layers.

If one considers individual hairpin vortices, the rapid development of the head and legs seems to either initiate along the direction of maximum strain (i.e. 45°) or move rapidly toward that angle of inclination after formation. Attainment of this

-13-

angle is indicated for the model in Figure 22d and can be roughly observed in the bubble-line patterns shown in Figures 14b and 18b. It is also worth noting that this same angle is demonstrated by the hairpin vortices generated by the hemisphere interaction (see Figures 17b and 18a). Obviously this behavior is not by pure happenstance since this stretching of hairpin-type vortices along the angle of maximum strain was originally suggested by Theodorsen (1952) and demonstrated by Head and Bandyopadhay (1981) as the characteristic angle of the hairpin vortices they observed in the outer region of turbulent boundary layers.

The generation of a series of "nested" hairpin vortices during the streak break down yields an important effect which bears upon the redevelopment of the low-momentum streak region. This effect is a process of apparent streamwise coalescence of the stretched legs of the multiple hairpins, as illustrated in Figure 22d. This process is speculative, but appears to occur, and supplies an explanation of how streaks maintain their integrity and persist both temporally and spatially. As shown in Figure 22d, the streamwise legs of multiple loops appear to coalesce in a three-dimensional fashion, with the legs of the older loops (which have been weakened by viscous effects) tending to orbit the more recent ones (see detail B-B in Figure 22d). The result is a continued agglomeration of the streamwise vorticity from the legs of individual vortex loops (which individually would be stretched and dissipated rapidly) into larger concentrations which will maintain their integrity and coherence in the presence of extreme stretching, external buffeting, and viscous dissipation. This process of coalescence and reinforcement of counter-rotating streamwise vorticity is felt to be the mechanism which was interpreted by Blackwelder and Eckelmann (1979) from anemometry studies as streamwise vortex pairs of extended length in the near-wall region, and as the cause of the temporal streak persistence [Smith and Metzler,1983; Section V. A above] and elongated streak patterns [Oldaker and Tiederman,1977] observed using visual methods.

Thus, with the movement of the hairpin vortices both downstream by convection and away from the surface by induction effects, the coalesced, streamwise remnants of the stretched legs remain behind, providing both elevated dissipation and a lateral accumulation of low-momentum fluid for either redevelopment of the bursting streak, or development of a new low-speed streak. Clearly, once the redevelopment process begins, it only requires the passage of another traveling pressure disturbance (probably the vortical remnant or agglomerated remnants from an upstream burst or bursts as suggested by Offen and Kline 1975) to set the streak bursting event off again. This brings the suggested streak bursting model full cycle.

VII. DISCUSSION

Clearly the present model hinges strongly on the formation of hairpin vortices as a key flow structure in the suggested near-well bursting event. The employment of this structure in the model is based not just on the kinematical observations of these and other studies, but also on the required dynamics of turbulent boundary layers in the near-wall. Several arguments for the necessary existence of such structures are as follows:

1) Turbulent flow requires an increased exchange of momentum with the wall in order to sustain the elevated shear stress levels in excess of a laminar, diffusion dominated flow. To accomplish this exchange of momentum, some active mechanism must develop within the boundary layer to act in essence as a "pump" to augment the removal of low momentum fluid from the wall [Lighthill,1963]. Three-dimensional vortex concentrations such as the hairpin vortex provide such a mechanism, acting as a pressure gradient pump near the wall (see Doligalski and Walker,1978), and as a transport vehicle carrying low-momentum fluid away from the wall due to mutual induction effects [Perry & Chong,1982; Bradshaw, 1978]. The suggested creation of hairpin vortices during the bursting event clearly

-14-

provides the necessary mechanism for transfer of low-momentum fluid both away from the wall and into the outer region. The inflow of high-momentum fluid toward the wall can be argued as both i) necessary to satisfy continuity and ii) the probable result of wallward induction effects created by the adjacent legs of flanking hairpin vortices.

2) As Bradshaw (1978) and Tennekes and Lumley (1972) (among others) point out, three-dimensional vortex stretching by the mean velocity gradient is necessary to sustain the energy transfer from the mean motion to the turbulent fluctuations. It is the present contention that the formation of hairpin vortices provides the logical mechanism for implementation of this energy transfer process in the near-wall, with the mean flow stretching process providing the energy input to the hairpins to sustain their role in the fluid, momentum, and energy exchange process.

3) The stretching of the legs of the hairpin also provides a clear mechanism for rapid elevation of energy dissipation levels in the near-wall. Clearly, during rapid stretching by the mean velocity gradient, the angular momentum in the legs of the hairpin (proportional to ωr^2) will be essentially conserved, while the energy (proportional to $\omega^2 r^2$) will grow as the vortex tubes narrow. The velocity gradients within the legs will also increase dramatically, which will strongly augment viscous dissipation in the vicinity of the wall as must occur in turbulent boundary layers.

4) Finally, as was discussed (Section II) and as has been illustrated (Figures 2, 3,4,5,19), low-speed streaks are the most organized, pervasive, and detectable structure within turbulent boundary layers despite the fact that they periodically break down and exist adjacent to the region demonstrating the highest turbulence levels. Since the streak is relatively benign, it is clear that its presence is indicative of a repetitive, causative agent of which the streak is the "foot print", as Nagawa and Nezu (1981) suggest. It is difficult to envision how flow structures spawned in the outer region of the boundary layer and approaching the near-wall could give rise to such organization. The alternative explanation is the repetitive generation of a near-wall flow structure whose characteristics must give rise to a perpetuation and re-development of the streak regions, and whose generation must be logically related to the existence of the low-speed streak regions. As demonstrated in the preceding model, the hairpin vortex structure satisfies these criteria.

Now, if such hairpin vortices are a mainstay of near wall turbulent behavior, why don't they clearly appear in the many previous visualization studies? There are several answers to this question. The first is that in visualization studies we can not directly visualize vorticity, but only the response of the visual indicator to the velocity field. In addition, many of the techniques employed utilize introduction of a medium (smoke or dye) which presents a picture of the history of the flow since introduction, not the active, local behavior. Second, we cannot visualize in three-dimensions. Thus we must attempt to interpret three-dimensional structures from two-dimensional pictures; a very difficult process since even simple three-dimensional flow structures can yield a plethora of different patterns, as illustrated by Figures 17, 18, 19, and 20. Finally, there is the problem that we are really dealing with idealizations of behavior, attempting to recognize symmetric and periodic behavior where in reality the behavior is neither, due to continued perturbation of a developing flow structure of interest by other similar flow structures in close proximity and with different phase relationships. Even when a discrete, periodic hairpin devoid of background disturbances does exist, the visualization and determination of its behavior

is still less than straightforward [e.g. Figure 17 and Perry et al.,1981].

When evaluated in comparison with the results of previous studies of near-wall behavior, the present model seems to be in general agreement. Clearly, all the elements for the burst event described by Kline et al. (1967) and Kim et al. (1971) are present in the model. The classic streak bursting sequence is summarized by Kline (1978) as consisting of lateral wall migration of low-speed fluid and streak formation, streak-lifting, oscillation, and breakup. All elements are present in the proposed model if one recognizes that as the hairpin vortices move outward with entrained low-speed streak fluid they will interact rapidly with previous vortical structures from parallel or upstream burst events, quickly creating a complex mire of three-dimensional vorticity. This latter behavior will rapidly mix dye/smoke/bubbles/particles to yield the appearance that the flow structure has "broken-up".

The rapid ejection event of Corino and Brodkey (1969) is equated in the present model to the streak entrainment by the hairpin vortices, as illustrated by Figures 22c and 22d. The relationship of this event to the "sweep" event they observe is suggested to be an inflow of higher momentum fluid in the wake of the hairpin burst event which passes to the lateral extremes of the streak as a result of flow induced toward the wall around the outside of the counter-rotating legs of the hairpins.

The model of the bursting event suggested by Offen & Kline (1975) is similar in many aspects to the present model, and acted as the stimulus for several of the studies reviewed previously. Indeed, if the combined hydrogen bubble-dye visualization sequences from their original report are examined [Offen & Kline, 1973], most of the essential elements of the present model can be observed, although the proper sequencing is difficult to discern due to slow spatial/temporal development of the flow structures at the low Reynolds numbers they examined.

Blackwelder (1978) in a model of the burst event, suggests that the interaction of a high-speed sweep with a low-speed streak creates an inflectional profile which gives rise to a growing oscillation of the shear layer between the sweep and the streak. Although not clearly apparent what causes the sweep inflow, he estimates (using inviscid, free shear layer considerations) that the oscillations of the streak should have a wavelength of roughly $\lambda_x^+ \doteq 150$. He supports this estimate by comparison with a series of visualization and probe studies which yield data suggesting wavelengths over a range of $120<\lambda_x^+<240$. Note the nondimensional spacing between hairpin vortices observed in the present study is 150 to 200 - in accord with Blackwelder's suggestion.

Since the initial description of the bursting process by Kline, several studies have attempted to establish methods for burst detection using single or multiple rakes of probes. If hairpin vortices are a part of the burst process, then it would seem that they should be detectable in the probe measurements. The difficulty is that the hairpin groups will not be generated in the same location or phase from burst event to burst event. Thus, a fixed, Eulerian probe cannot hope to do an appropriate job of detection of such structures. In addition, since the number of hairpins will vary from burst to burst, the number of cycles in the velocity signature will vary, creating further confusion in our symmetry/periodicity atuned minds. However, to illustrate that signals potentially characteristic of hairpin vortex groups are present in anemometry signals taken in the near-wall, consider the velocity signals from a hot-wire rake shown by Blackwelder and Kaplan (1976) in their Figures 7 and 8, or in Figure 1 and Figure 5 (temperature measurements) from Blackwelder (1978). A close examination of these signals indicates that at sporadic intervals, somewhat periodic oscillations occur in packet-like bunches of 2 to 5 oscillations. Although of irregular amplitude and appearing anywhere from $5<y^+<100$ (as might be expected since the structures both influence the wall and are carried away from it), oscillation periods of $10<t^+<20$ appear to be a recurrent characteristic. If we assume these oscillations to have a characteristic non-dimensional wavelength of λ_x^+ and to move past the probe at the

convection velocity for hairpin vortices indicated in Section IV.C above, $u_c = 13.1\, u_\tau$, we can write:

$$\lambda_x^+ = u_c^+ t^+ = 13.1t^+$$

this yields a range of estimated wavelengths of $132 < \lambda_x^+ 264$ which is again essentially the range of observed spacing of the hairpin structures.

The present study has concentrated on the near-wall flow behavior, with only cursory attention to the outer region. Clearly, as Kline (1978) points out, the two must interact. One question that arises is what happens to the hairpin structures once they leave the near-wall? The present suggestion is that they begin to interact with vortex structures from previous and parallel burst events, either reinforcing one another by vortex coalescence or dying by mutual vorticity cancellation as described by Perry and Chong (1982). Reinforcement should yield larger scales and motions as are observed in the outer region pictures of Figure 13. Support for this type of growth process from the interconnected groups of hairpin vortices generated in the near-wall is illustrated by the apparent maintenance of both the "linked" structure appearance and the characteristic 15° to 30° projection angles with the wall far beyond the near-wall region.

VIII. FINAL COMMENTS

The model of the near-wall flow behavior presented in this paper is a synthesis from a number of inputs, with a strong bias placed on the author's past and present research. Although stated in a definitive manner, the model is obviously a hypothesis of the near-wall behavior, and like all hypotheses must await confirmation/negation/modification. I do feel that the proposed model provides a physically logical sequence of events which expalins many of the observations/measurements for the near-wall region. Clearly, like the archaeologist, I have tried to recreate a "beast" of the turbulence jungle based on the bits of remains, tracks, and droppings of which I have knowledge. And as in the search for all beasts which we have yet to capture and tame, I'm hopeful that my present model helps guide the hunt and facilitates its eventual domestication.

IX. ACKNOWLEDGEMENTS

X. REFERENCES

1. Acarlar, M.S. and Smith, C.R. (1984). in preparation.

2. Achia, B.U. & Thompson, D.W. (1976). J. Fluid Mech.,81, 439.

3. Bakewell, H. and Lumley, J.L. (1967). Phys. Fluids,10, 1880.

4. Blackwelder, R.F. (1978). ibid Ref. 41, 98.

5. Blackwelder, R.F. and Kaplan, R.E. (1976). J. Fluid Mech.,76, 89.

6. Blackwelder, R.F. and Eckelmann, H. (1979). J. Fluid Mech.,94, 577.

7. Bradshaw, P. (1972). Chap. 1 in Turbulence, Topics in Applied Physics, Vol. 12 (ed. P. Bradshaw), Springer-Verlag, pp. 9-13.

8. Brodkey, R.S. and Wallace, J.M. (1982). The Delta Conferences, NSF Project Report, The Ohio State Research Foundation, Columbus,Ohio.

(continued)

X. REFERENCES (continued)

9. Brown, G.L. and Thomas, A.S.W. (1977). Phys. Fluids 20, S243.

10. Cantwell, B.(1981). Annual Review of Fluid Mechanics, 13, 457.

11. Cantwell, B., Coles, D. and Dimotakis, P.(1977). J. Fluid Mech.,87, 641.

12. Corino, E.R. and Brodkey, R.S. (1969). J. Fluid Mech.,37, 1.

13. Danberg, J.E. (1978). ibid Ref. 41, 429.

14. Doligalsi, T.L, and Walker, J.D.A. (1978). ibid Ref. 41, 288.

15. Falco, R.E. (1978). ibid Ref. 41, 448.

16. Falco, R.E. (1981) Proceedings of Sixth Symposium on Turbulence in Liquids (ed. G.K. Patterson and J.L. Zakin), Dept. of Chem. Engrg., University of Missouri-Rolla,1.

17. Head, M.R. and Bandyopadhyay, P. (1981). J. Fluid Mech.,107, 297.

18. Hinze, J.O. (1975) Turbulence, 2nd edn., McGraw-Hill, pp. 682-683.

19. Johansen, J.B. and Smith, C.R. (1983). Report FM-3, Dept. of Mech. Engrg. & Mech., Lehigh University, Bethlehem, PA.

20. Kim, H.T. Kline, S.J. and Reynolds, W.C. (1971). J. Fluid Mech.,50, 133.

21. Kline, S.J. (1978). ibid Ref. 41, 1.

22. Kline, S.J., Reynolds, W.C., Schraub, F.A. and Runstadler, P.W. (1967). J. Fluid Mech.,30, 741.

23. Kline, S.J. and Falco, R.E. (1980). Summary of AFOSR/MSU Research Specialists Workshop on Coherent Structure in Turbulent Boundary Layers, AFOSR TR-80-0290, Dept. of Mech. Engrg., Michigan State Univ., East Lansing, MI.

24. Kreplin, H.P. and Eckelmann, H. (1979). J. Fluid Mech, 95, 305.

25. Lee, M.K., Eckelman, L.D., and Hanratty, T.J. (1974). J. Fluid Mech., 66, 17.

26. Lighthill, M.J. (1963). in Laminar Boundary Layers (ed. L. Rosenhead), Clarendon Press, Oxford. pp. 98-99.

27. Metzler, S.P. (1981) Processes in the Wall Region of a Turbulent Layer. M.S. Thesis, Dept. of Mech. Engrg. & Mech., Lehigh University, Bethlehem, PA.

28. Moin, P. and Kim, J. (1982). J. Fluid Mech., 118, 341.

29. Nagib, H.M. Guezennec, V., and Corke, T.C. (1978). ibid Ref. 41, 372.

30. Nakagawa, H. and Nezu, I. (1981). J. Fluid Mech., 104, 1.

31. Nychas, S.G., Hershey, H.C. and Brodkey, R.S. (1973). J. Fluid Mech.,61, 513.

32. Offen, G.R. and Kline, S.J. (1973). Experiments on the velocity characteristics of "bursts" and in the interactions between the inner and outer regions of a turbulent boundary layer, Report MD-31, Stanford University.

33. Offen, G.R. and Kline, S.J. (1975). J. Fluid Mech., 70, 209.

34. Oldaker, D.K. and Tiederman, W.G. (1977). Phys. Fluids,20, S133.

35. Perry, A.E. and Chong, M.S. (1982). J. Fluid Mech., 119, 173.

36. Perry, A.E., Lim, T.T., and Teh, E.W. (1981). J. Fluid Mech., 104, 387.

37. Praturi, A.K. and Brodkey, R.S. (1978). J. Fluid Mech.,89, 251.

38. Rosenhead, L. (1932). Proc. Roy. Soc. London, A134, 170.

39. Schwartz, S.P. (1981). Investigation of Vortical Motions in the Inner Region of Turbulent boundary layer. M.S. Thesis, Dept. of Mech. Engrg. & Mech., Lehigh University, Bethlehem, PA.

40. Smith, C.R. (1978) ibid Ref. 41, 48.

41. Smith, C.R. and Abbott, D.E. (eds.) (1978). Coherent Structure of Turbulent Boundary Layers, AFOSR/Lehigh University Workshop

X. REFERENCES (continued)

42. Smith, C.R. and Metzler, S.P. (1982). in
    Developments in Theoretical and Applied
    Mechanics, Vol. XI (ed. T.J. Chung & G.R.
    Karr), Dept. of Mech. Engrg., University
    of Alabama in Huntsville, 533.

43. Smith, C.R. and Metzler, S.P. (1983). J. Fluid
    Mech., 129, 27.

44. Smith, C.R. and Schwartz, S.P. (1983). Phys.
    Fluids, 26 (3), 641.

45. Theodorsen, T. (1952). Proc. 2nd Midwestern
    Conf. on Fluid Mech., Ohio State Univ.,
    Columbus, Ohio.

46. Utami, T. and Ueno, T. (1979). in Flow
    Visualization (ed. T. Asanunra), Hemisphere,
    221.

47. Wallace, J.M. (1982). ibid. Ref. 42, 509.

48. Willmarth, W.W. (1975). Adv. Appl. Mech.,15,
    159.

49. Willmarth, W.W. (1978). ibid Ref. 41, 130.

50. Willmarth, W.W. and Tu, B.J.(1967). Phys.
    Fluids,10, S134.
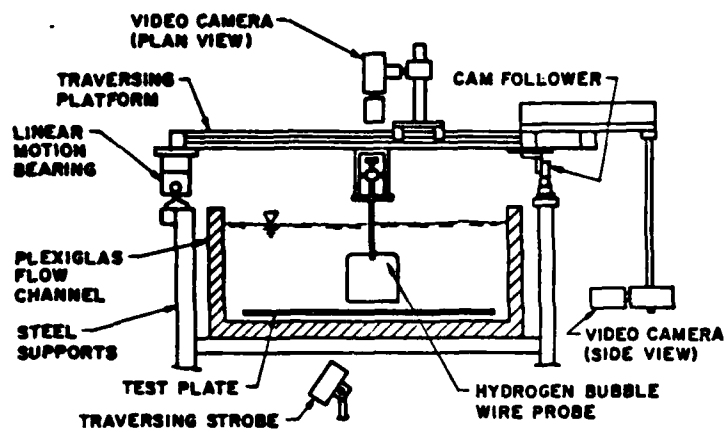
Figure 1. Cross Section of free-surface water channel
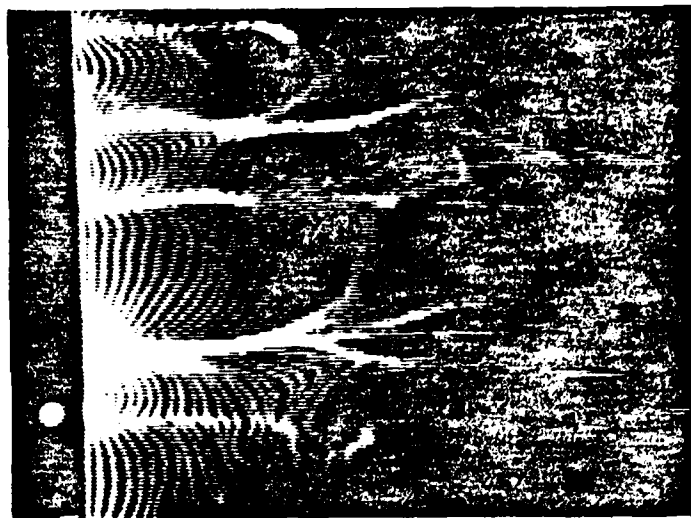
Figure 2. Top-view of low-speed pattern. $Re_\theta = 4180$. (Flow left to right).
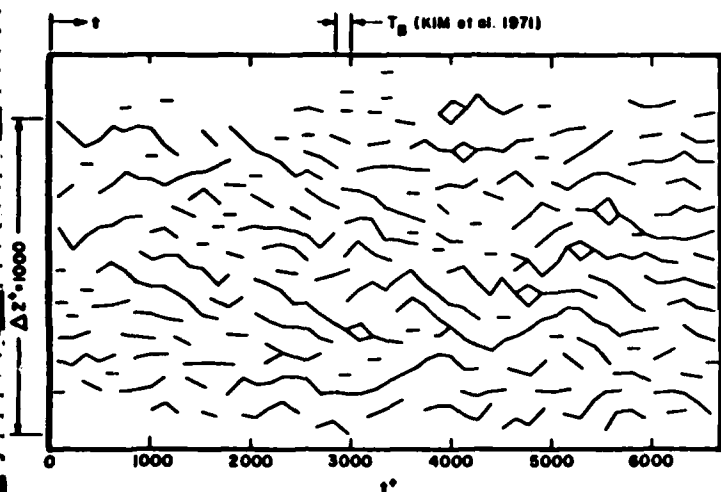
Figure 3. Graph indicating temporal persistence of streaks (from Smith & Metzler 1983).
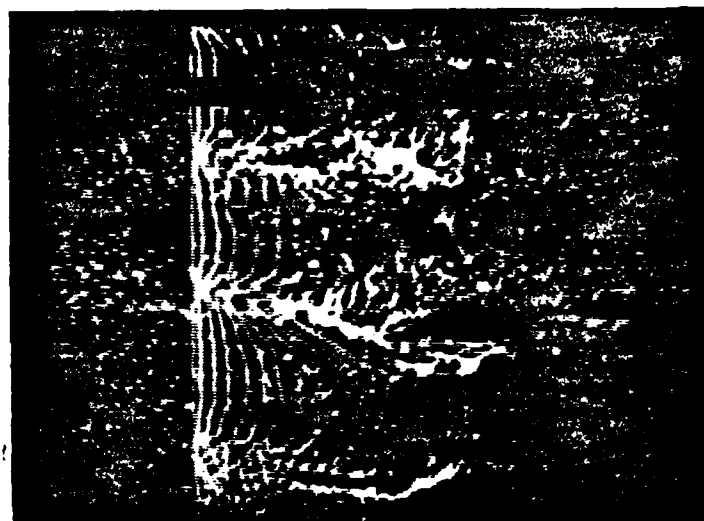
Figure 4. Bead aggregations in coincidence with low-speed streaks, $Re_\theta = 2250$.
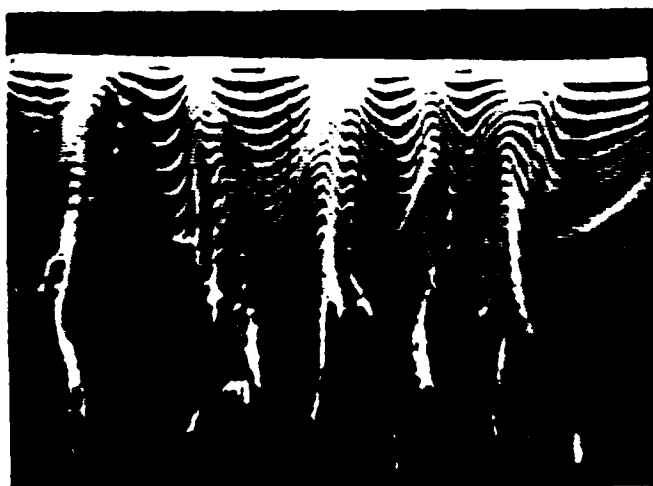
a) No rods. $y^+ = 5$
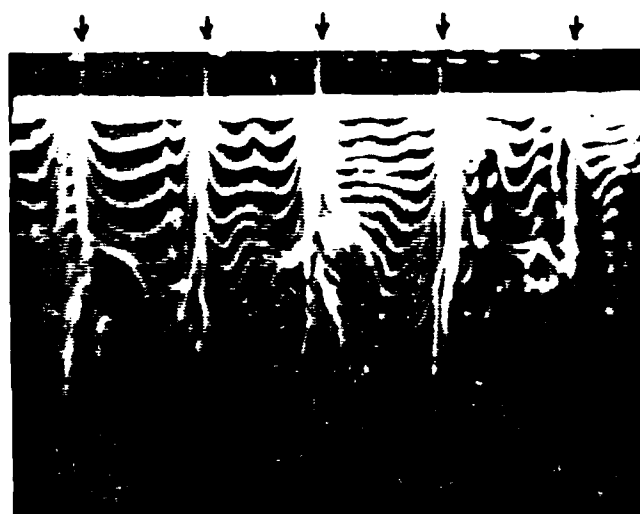
b) Rods spaced $s^+ = 71$. $y^+ = 5$.

Figure 5. The focusing effect of sublayer-scale streamwise rods on low-speed streaks. positions of rods indicated by arrows. $Re_\theta = 1500$. (Flow top to bottom).
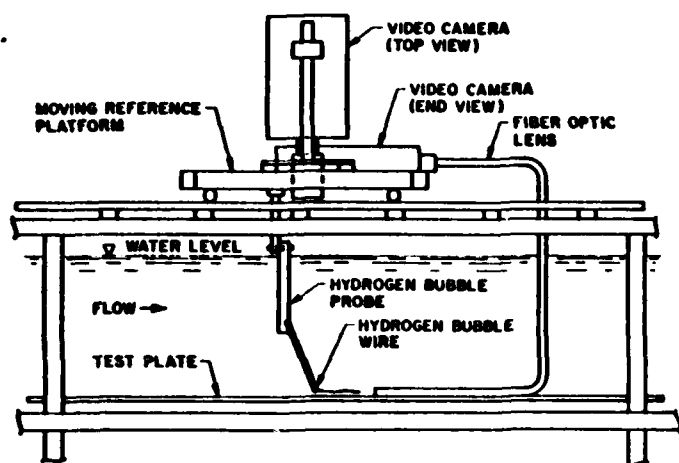
a) Visualization system schematic   b) Top-end view display technique
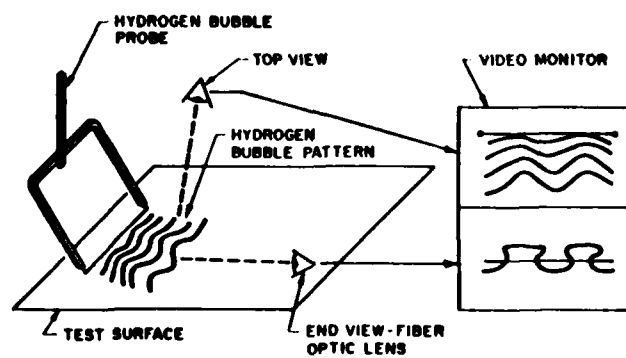
Figure 6.   Schematic of system configuration and display of top-end views
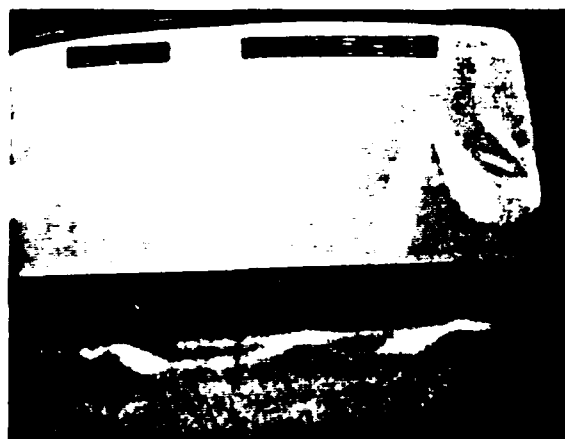
a) $t^+ = 0$ b) $t^+ = 14$

Figure 7.   Top-end view of streak upwelling and "mushrooming" effect. $Re_\theta = 1700$, $y^+ = 14$.
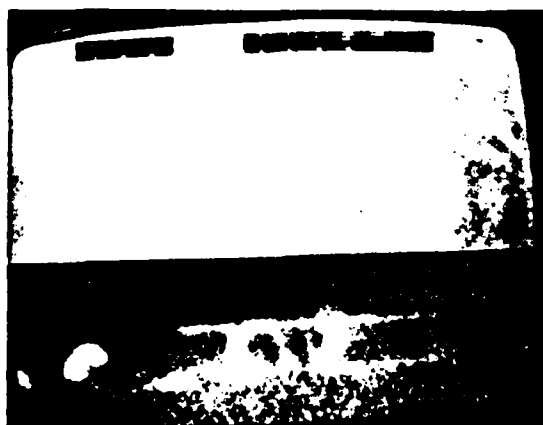
a) $t^+ = 0$ b) $t^+ = 16$

Figure 8.   Top-end view of counter-rotating vortex pattern. $Re_\theta = 1700$, $y^+ = 14$.
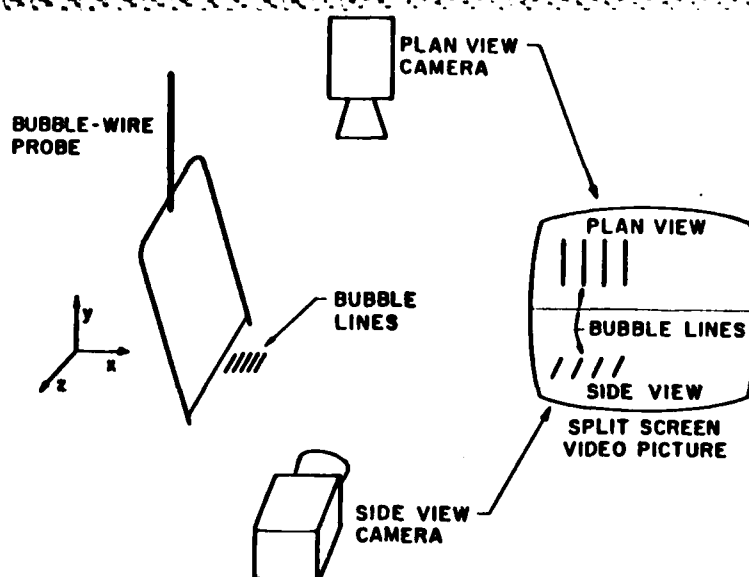
Figure 9.   System configuration for combined top-side view studies.

a) "kinked" streak, $y^T = 15$
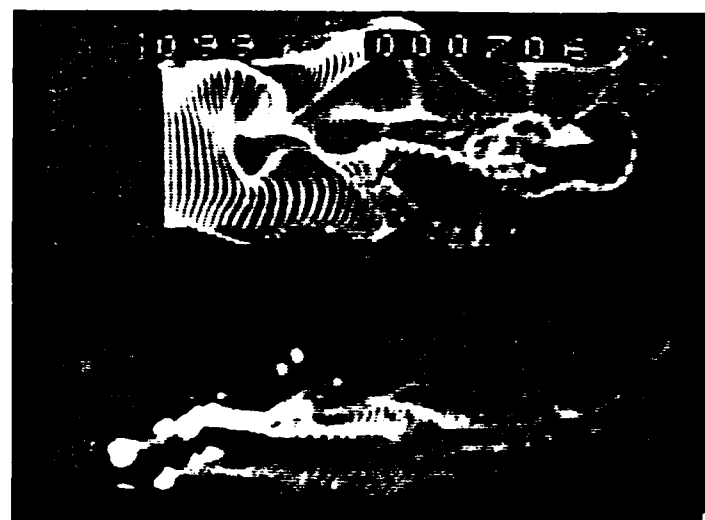
b) "Bulged" streak breakdown, $y^+ = 15$

Figure 10.   Top-side views illustrating streak behavior during breakdown. $Re_\theta = 1910$.
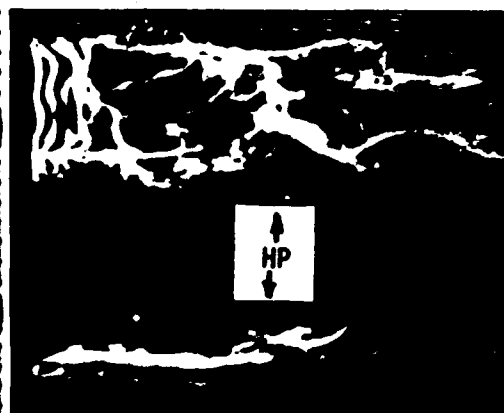
a) $t^+ = 0$
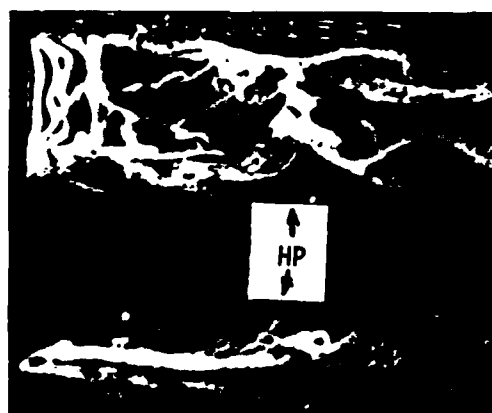
b) $t^+ = 2$
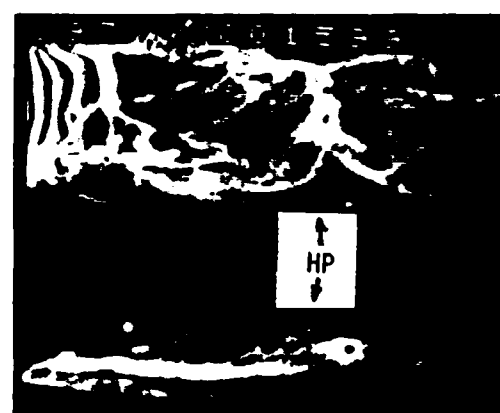
c) $t^+ = 4$

Figure 11.   Top-side view sequence of hair-pin vortex formation/appearance in near-wall of turbulent boundary layer. $Re_\theta = 1910$, $y^+ = 5$.
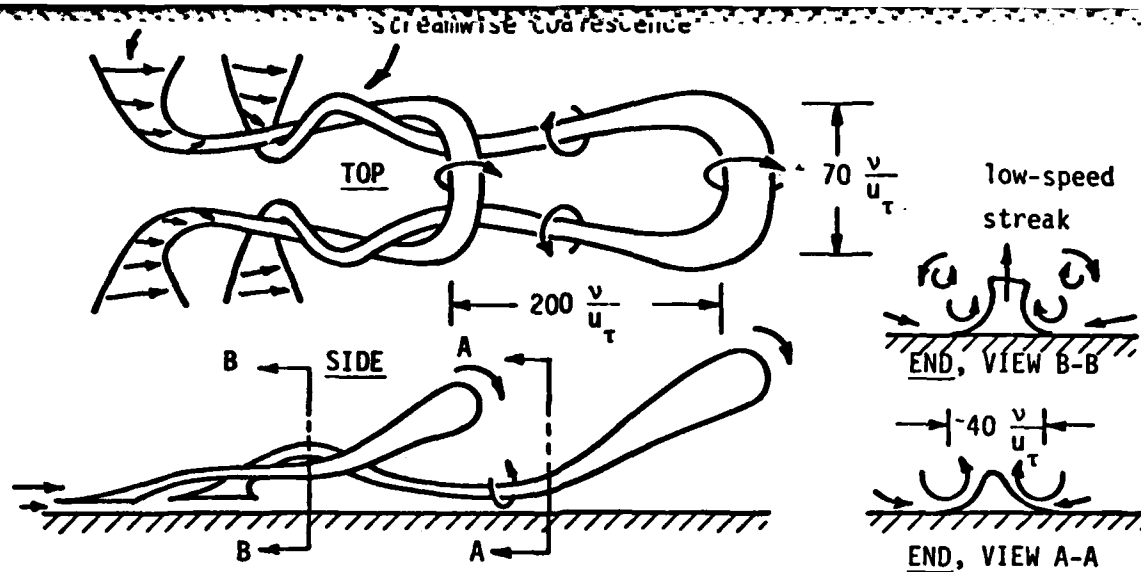
Figure 12. Schematic of combined hair-pin vortex flow structure suggested by top-side view studies.
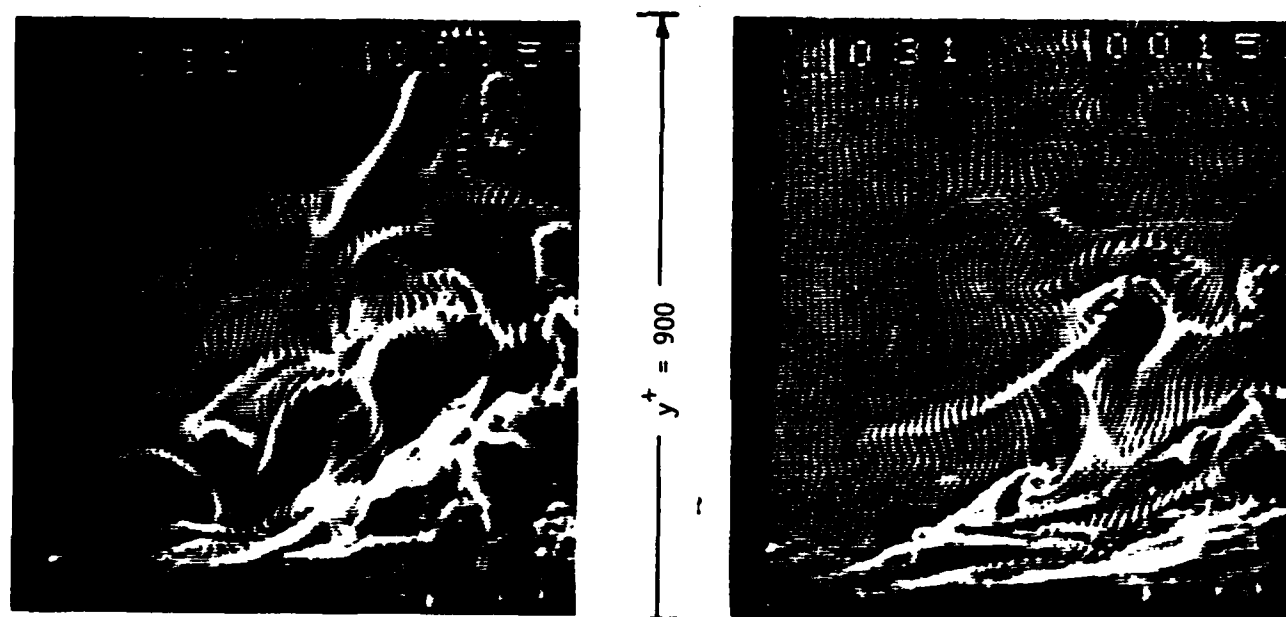
Figure 13. Side-view of turbulent boundary layer. Re_θ = 2200 (Flow left to right).

a) $t^+ = 22$ b) $t^+ = 0$
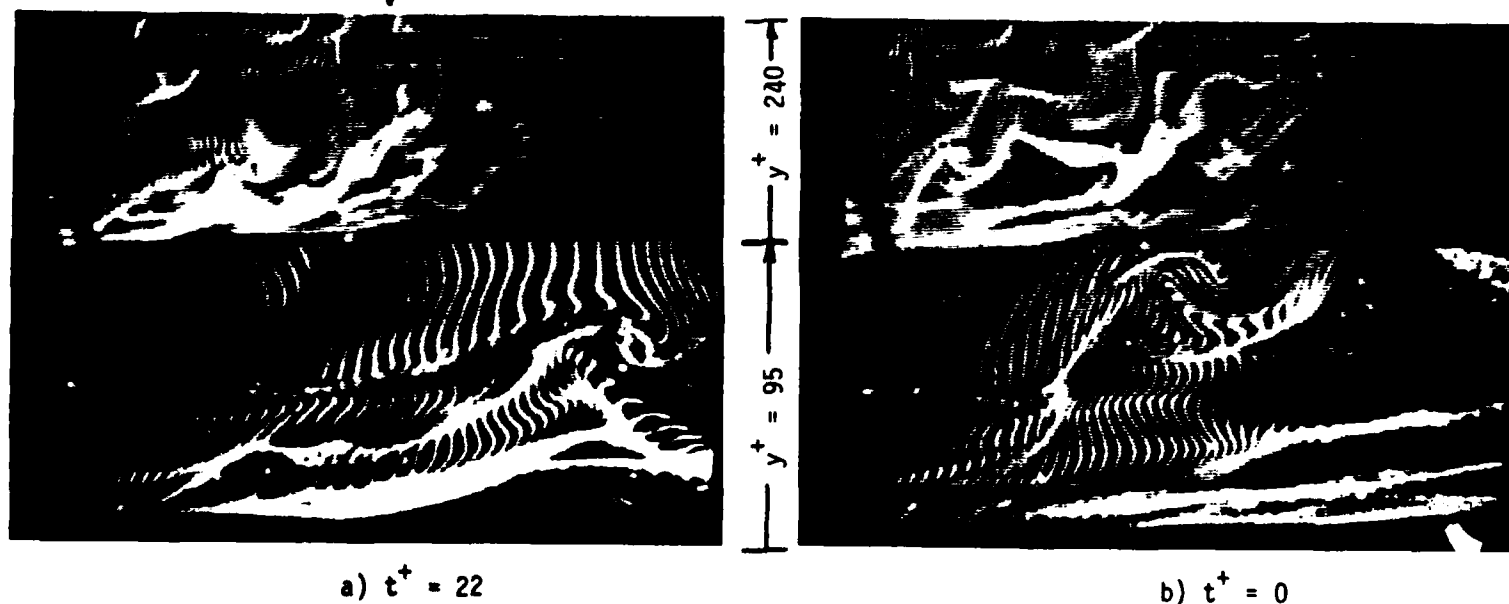
Figure 14. Combined side-view pictures of turbulent boundary layer. Lower picture is magnified view of near-wall flow structure in lower left of upper picture. Re_θ = 2200.
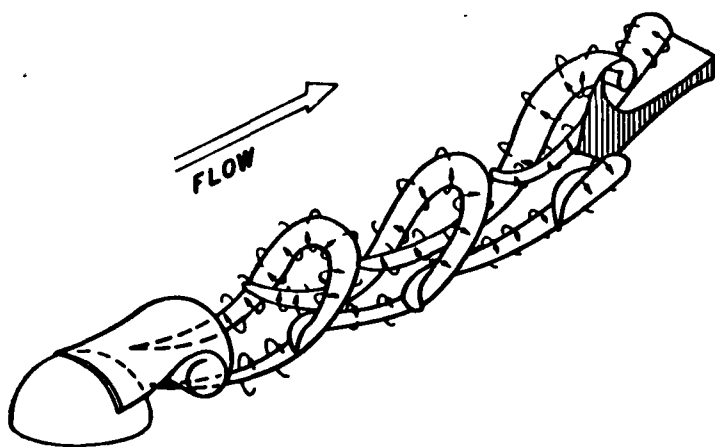
Figure 15.   Schematic illustrating hair-pin vortex formation in wake of hemisphere.
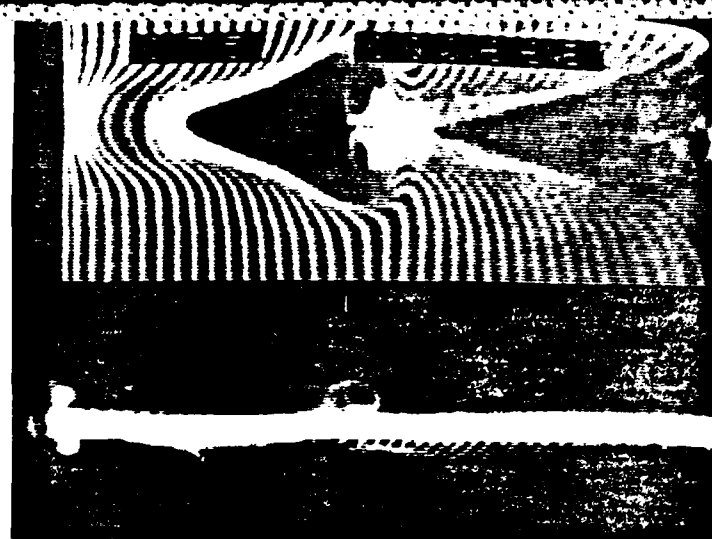
a) $y_{wire}/R = 0.75$

b) $y_{wire}/R = 0.5$

Figure 16.   Side-view visualization revealing head of hair-pin vortex in wake of hemisphere.
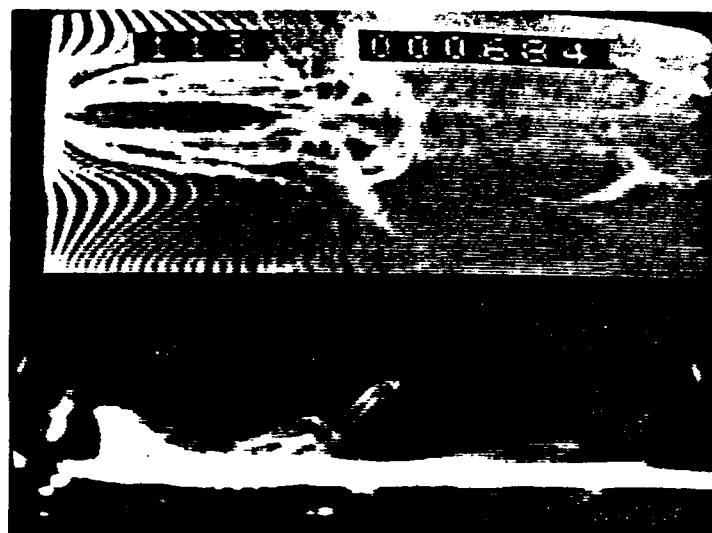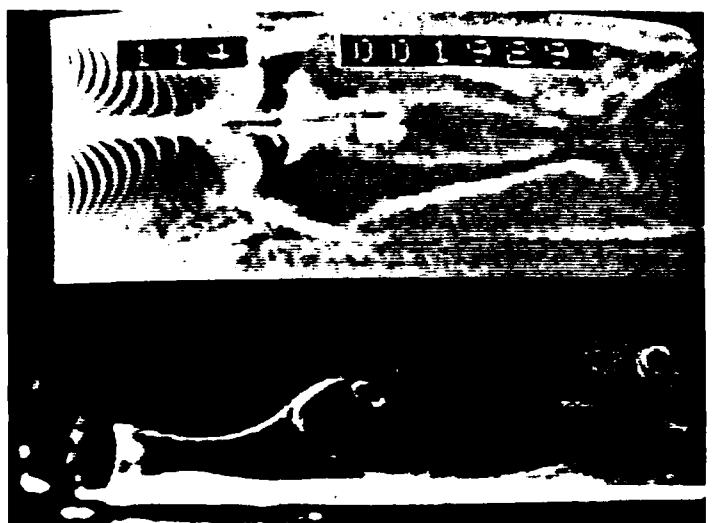
c) $y_{wire}/R = 0.25$

Figure 17.   Top-side view patterns created by hair-pin vortices with bubble-wire at $X/R = 5$ from rear of hemisphere.
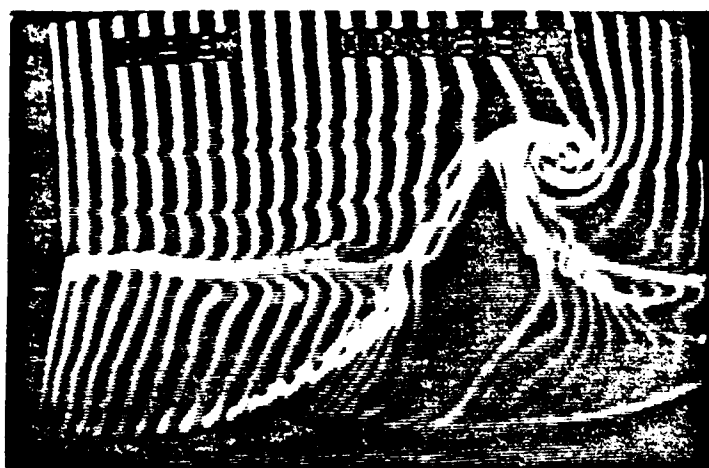
a) Hair-pin vortex, X/R = 20
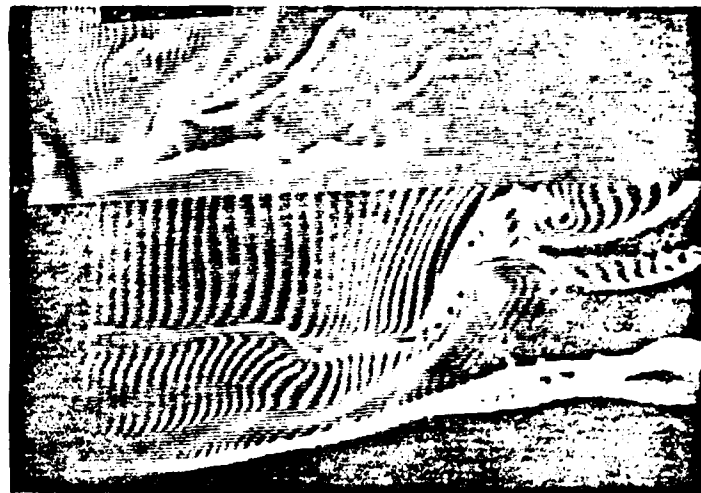
b) Turbulent boundary layer, Re_θ = 2200

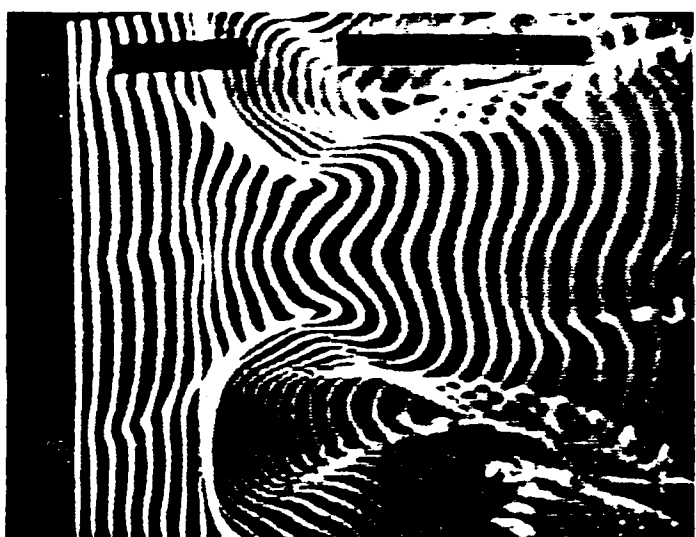Figure 18. Side-view comparison between hair-pin vortex and turbulent boundary layer patterns.
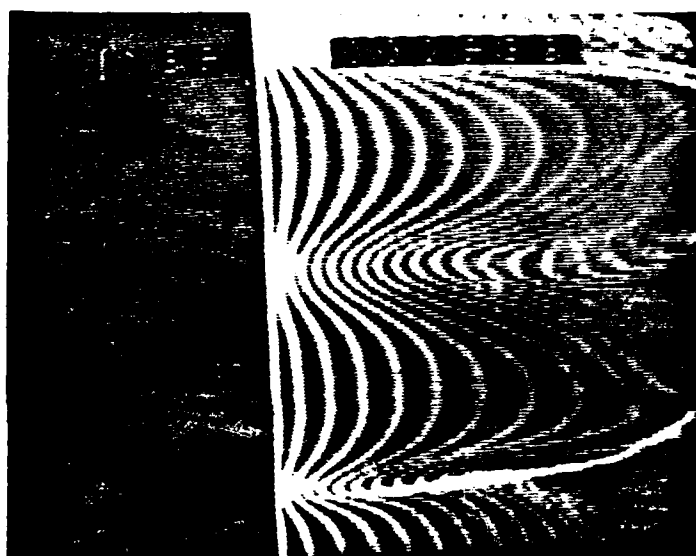
a) Hair-pin vortex, X/R = 20, y_{wire}/R = 0.08
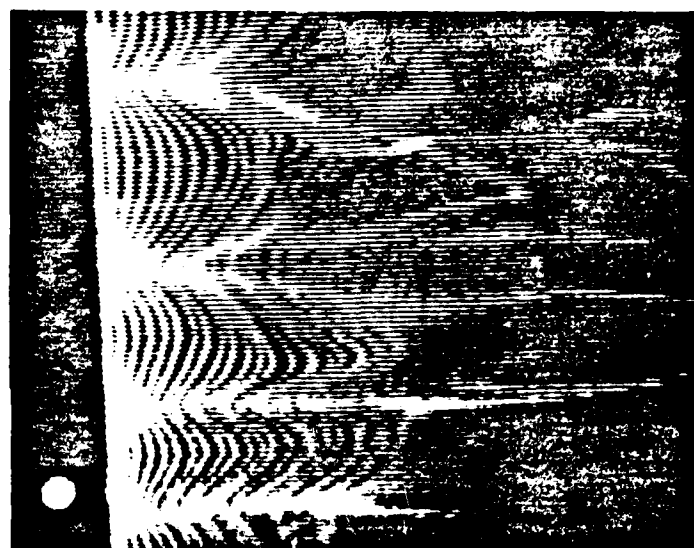
b) Turbulent boundary layer, Re_θ = 2200, y_{wire}^+ = 5

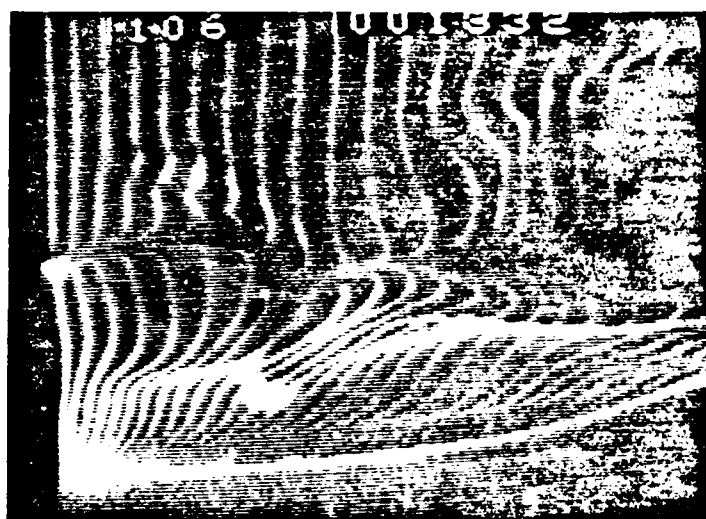Figure 19. Top-view comparison between hair-pin vortex and turbulent boundary layer pattern.

a) Hair-pin vortex, X/R = 20, y_{wire}/R = 0.25
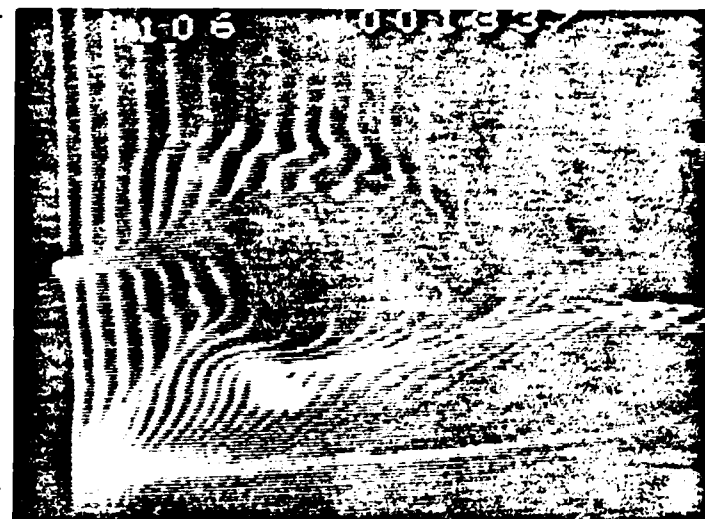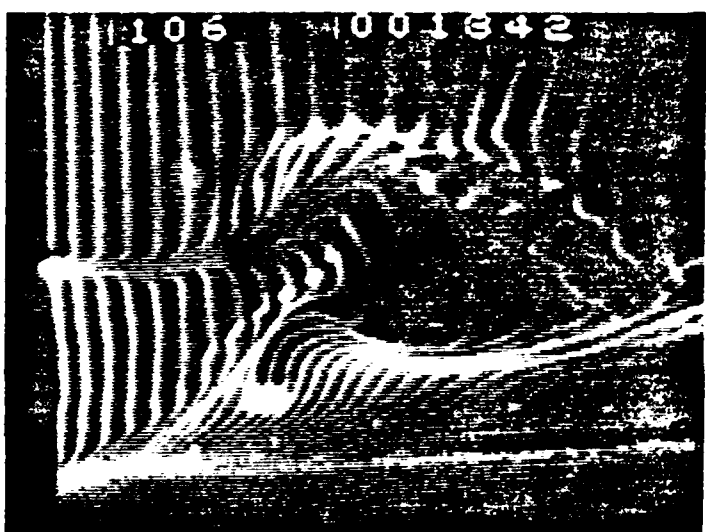
Figure 20. (See Figure 19 caption)

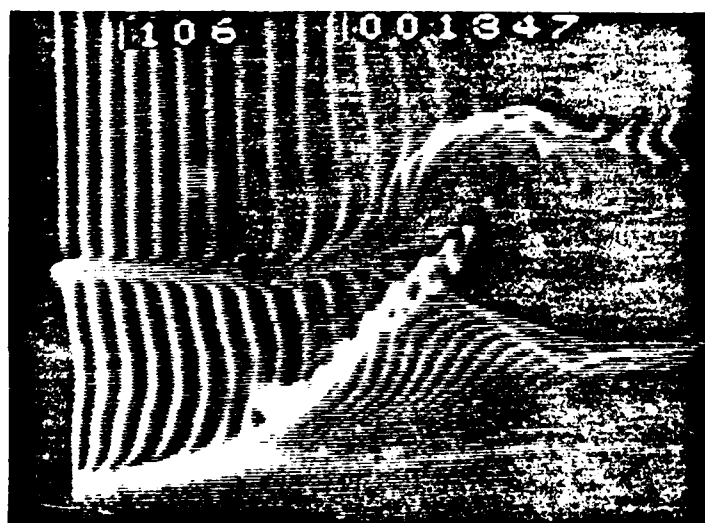b) Turbulent boundary layer, Re_θ = 2200, y_{wire}^+ = 30
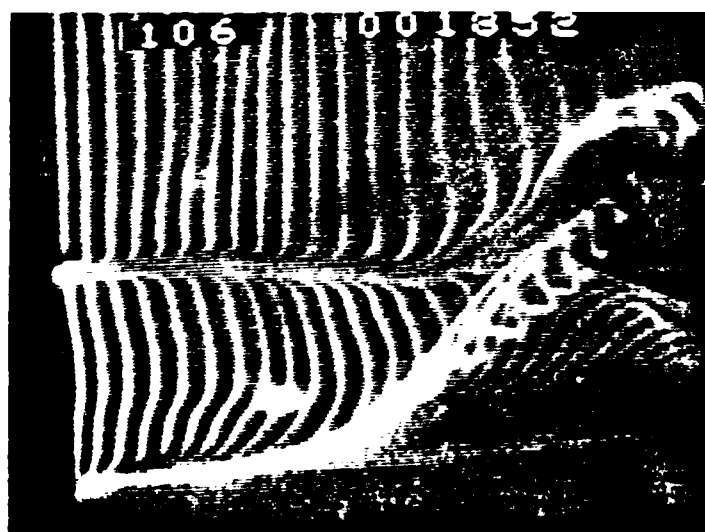
a) $t^+ = 0$

b) $t^+ = 2$

c) $t^+ = 4$

d) $t^+ = 6$

e) $t^+ = 8$

Figure 21. Side-view sequence in near-wall turbulent boundary layer showing the breakdown of an inflectional velocity profile into a hair-pin vortex. Note the 45° angle of the legs of the vortex. $Re_\theta = 1700$.

TOP VIEW

Low-Speed Streak   Lift-up & Oscillation   Flow ⟶

SIDE VIEW

a) lift-up and oscillation

Vortex roll-up

$y^+ \approx 15\text{-}30$

b) initiation of vortex roll-up

"hair-pin" vortex

Upward movement due to mutual induction

Vorticity "Sheet"

$y^+ \approx 50\text{-}100$

$\Delta z^+ \approx 40$

A

A

END, VIEW A-A

c) vortex development: amplification and concentration

Streamwise Vortex Stretching

Streamwise Coalescence

$\Delta x^+ = 150 \text{ to } 200$ $\approx 45°$

$15°$ to $30°$

$y^+ > 100$

B

B

END, VIEW B-B

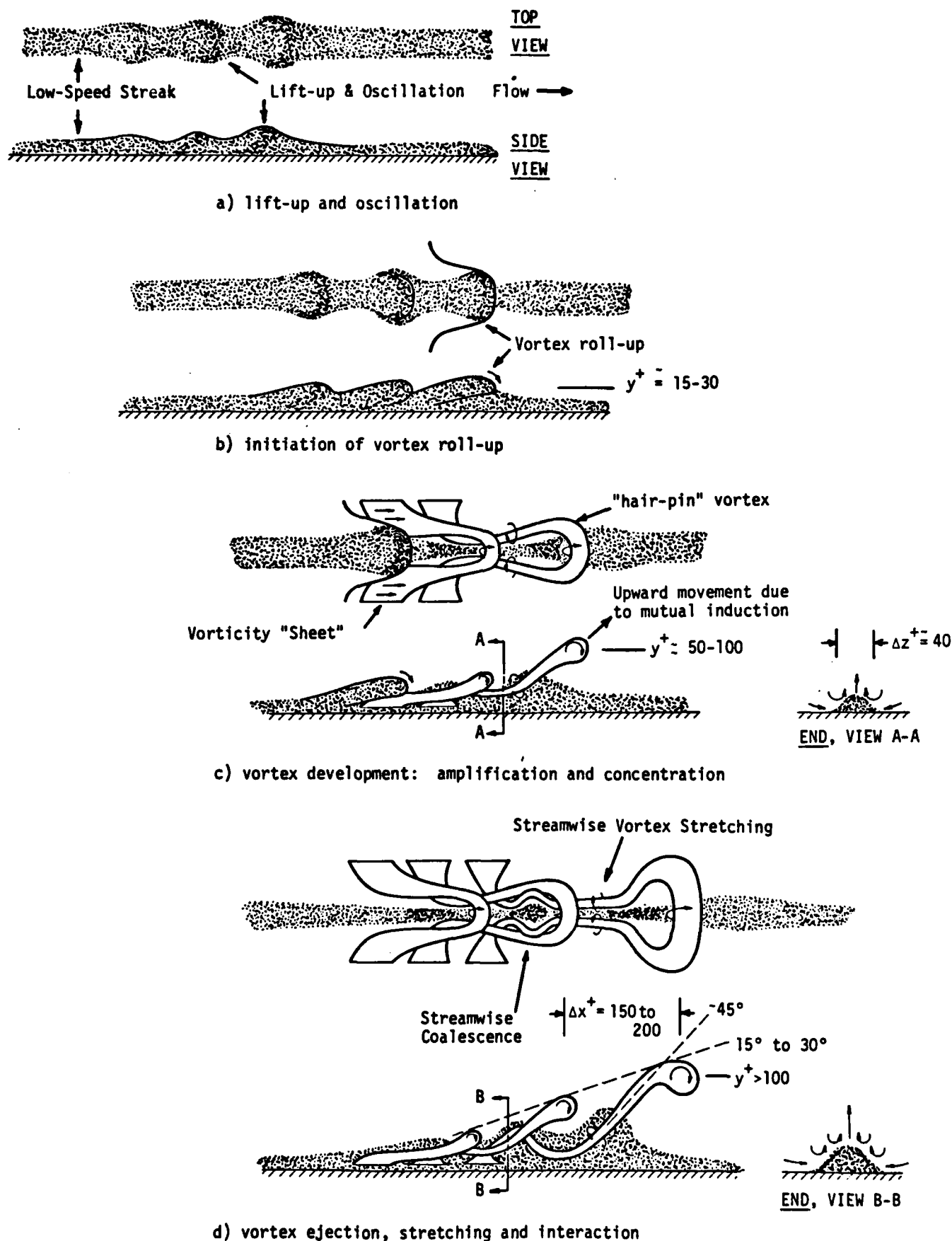**d) vortex ejection, stretching and interaction**

Figure 22.   Illustration of the breakdown and formation of hairpin vortices during a streak "bursting" process. Low-speed "streak" regions indicated by shading.

END

FILMED

2-84

DTIC